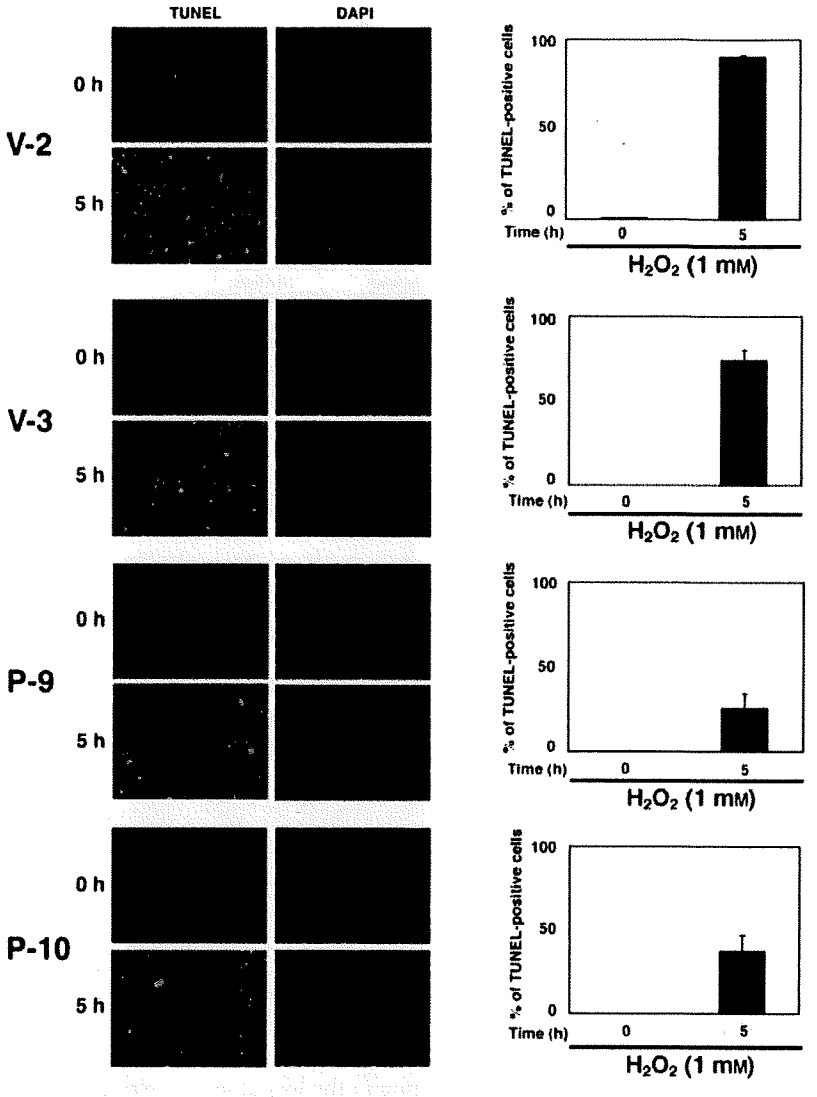

Figure 4 p53 is required for the H_2O_2-induced apoptosis in Huh6 cells. TUNEL staining. The indicated cell clones were treated with H_2O_2 at a final concentration of 1 mM or left untreated. Five hours after the treatment with H_2O_2, apoptotic cells were identified by TUNEL assay as described under Experimental procedures. The cell nuclei were stained with DAPI (left panels). The number of TUNEL-positive cells was counted, and expressed as a percentage of the total number of cells examined (right panels). H_2O_2-induced apoptosis was significantly different in cells expressing siRNA against p53 as compared with control cells. $P < 0.05$.

cytoplasmic/nuclear fractions were prepared and subjected to RT-PCR and Western blotting with the anti-Parc antibody, respectively. As shown in Fig. 6B, siRNA against Parc successfully reduced the expression levels of the endogenous Parc. Unexpectedly, siRNA-mediated knock-down of the endogenous Parc had a negligible effect on the subcellular localization of p53 in Huh6 cells as examined by Western blotting (Fig. 6C).

Nicotinamide treatment inhibits the H_2O_2-mediated nuclear translocation of p53 and apoptosis

Recently, it has been shown that the chemical modifications including acetylation regulate the subcellular localization of p53 (Kawaguchi *et al.* 2006). We then examined a possible effect of histone deacetylase inhibitor nicotinamide (Nico) on the H_2O_2-mediated nuclear translocation of p53 and p53-dependent apoptotic cell death. To this end, Huh6 cells were treated with the indicated combinations of drug. At the indicated time periods after the treatment, cells were biochemically fractionated into cytoplasmic and nuclear fractions, and subjected to Western blotting with the anti-p53 antibody. As shown in Fig. 7A, nicotinamide significantly inhibited the H_2O_2-mediated nuclear translocation of p53. Next, we sought to address whether nicotinamide could affect the H_2O_2-induced apoptosis. For this purpose, Huh6 cells were exposed to the indicated combinations of drug, and the number of TUNEL-positive cells was measured. As shown in Fig. 7B, nicotinamide treatment markedly inhibited

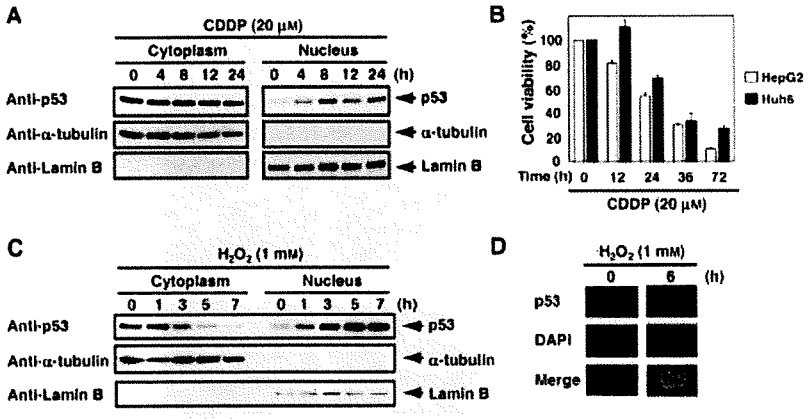

Figure 5 Nuclear translocation of p53 in response to H_2O_2. (A) CDDP-induced nuclear accumulation of p53. Huh6 cells were treated with 20 μM of CDDP. At the indicated time points after the treatment, cells were collected and fractionated into cytoplasmic and nuclear fractions, followed by Western blotting with the indicated antibodies. (B) CDDP-induced apoptotic cell death of Huh6 cells. At the indicated time periods after the exposure to CDDP (20 μM), Huh6 cells were subjected to MTT assay. (C) H_2O_2-mediated nuclear translocation of p53 in Huh6 cells. At the indicated time periods after the treatment with H_2O_2 (1 mM), Huh6 cells were fractionated into cytoplasmic and nuclear fractions, and subjected to Western blotting with the indicated antibodies. (D) Indirect immunofluorescence. Huh6 cells were treated with H_2O_2 (1 mM) or left untreated, and stained with anti-p53 antibody (red). Cells were costained with DAPI (blue) to reveal cell nucleus.

the H_2O_2-induced apoptotic cell death as compared with H_2O_2 alone. Similar results were also obtained in MTT assays (Fig. 7C). Together, our results strongly suggest that the acetylation status might be critical for the H_2O_2-induced nuclear translocation of p53 and apoptosis in HBL cells.

Discussion

p53 acts as a tumor suppressor by inducing cell cycle arrest and/or apoptotic cell death in tumor cells. It has been well documented that p53 mutation is found in over 50% of all human tumors, resulting in the loss of its pro-apoptotic function (Hollstein *et al.* 1991; Vogelstein *et al.* 2000). The pro-apoptotic function of p53 can be also abrogated by non-mutational mechanisms (Prives & Hall 1999). For example, p53 is infrequently mutated in human NBL; however, p53 is largely localized in cytoplasm, indicating that p53 has no role in the genesis and development of NBL (Vogan *et al.* 1993). Like NBL, extensive studies on the p53 status demonstrated the absence of mutations in HBL (Chen *et al.* 1995; Ohnishi *et al.* 1996). Although β-catenin is frequently mutated in HBL (Koch *et al.* 1999; Takayasu *et al.* 2001), recent studies suggest that β-catenin mutation alone is not sufficient for hepatocarcinogenesis (Harada *et al.* 2002; Harada *et al.* 2004). In the present study, we have found that p53 is exclusively expressed in cytoplasm of human primary HBL as well as HBL-derived Huh6 cells. In response to oxidative stress, p53 was translocated into cell nucleus, and exerted its pro-apoptotic function. Intriguingly, histone deacetylase inhibitor treatment strongly inhibited the oxidative stress-induced nuclear access of p53. Thus, it is likely that the cytoplasmic retention of p53, which might be mediated by acetylation, contributes at least in part to the genesis and development of HBL.

As mentioned above, the previous studies demonstrated that wild-type p53 is significantly accumulated in cytoplasm of human NBL (Moll *et al.* 1995; Ostermeyer *et al.* 1996). According to their results, the treatment of NBL-derived cells with p53 COOH-terminal peptide resulted in the relocalization of p53 to the cell nucleus, suggesting that the COOH-terminal region of p53 contributes to its cytoplasmic retention. As described (Stommel *et al.* 1999), p53 shuttles between cell nucleus and cytoplasm in its potential COOH-terminal nuclear export signal (NES) and its receptor Crm-1-dependent manner. Based on our present results, however, the nuclear export inhibitor LMB treatment had undetectable effect on the subcellular localization of p53 in Huh6 cells, suggesting that the NES-mediated efficient nuclear export is not involved in a significant cytoplasmic accumulation of p53 in Huh6 cells. Nikolaev *et al.* (2003) found that Parc prevents the nuclear translocation of p53 through the interaction with its lysine-rich COOH-terminal region which contains the nuclear localization signals (NLSs), and also suggested that their interaction might be regulated by post-translational modifications of p53 such as phosphorylation and/or

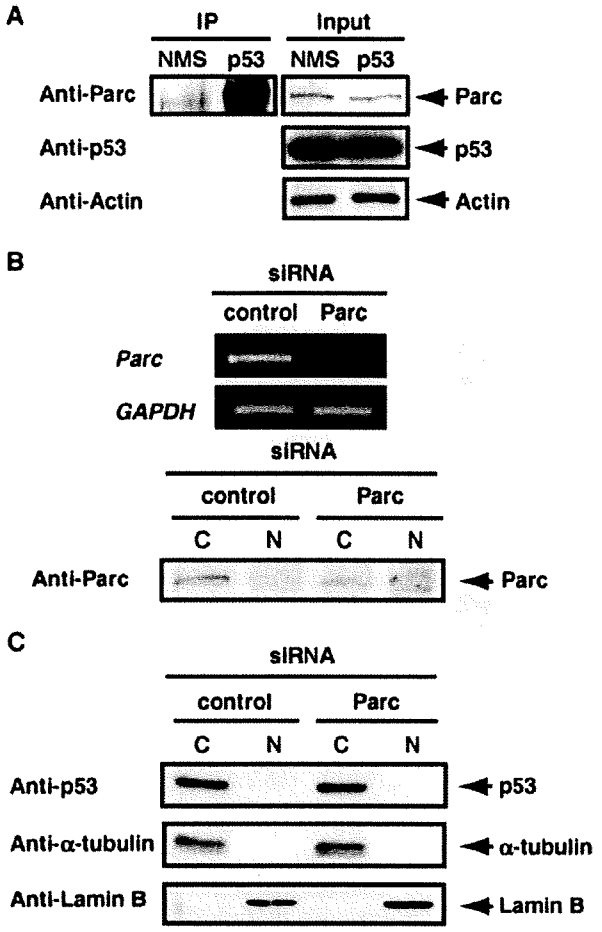

Figure 6 Parc has an undetectable effect on the subcellular localization of p53. (A) Parc is associated with p53 in Huh6 cells. Whole cell lysates prepared from Huh6 cells were immunoprecipitated with normal mouse serum (NMS) or with the anti-p53 antibody. The immunoprecipitates were analyzed by Western blotting with the anti-Parc antibody. Input corresponds to 5% of the whole cell lysates used in this assay. (B) siRNA-mediated knockdown of the endogenous Parc. Huh6 cells were transiently transfected with siRNA against Parc or with the control siRNA. Twenty-four hours after transfection, total RNA and cytoplasmic (C) nuclear (N) fractions were prepared and processed for RT-PCR and Western blotting with the anti-Parc antibody, respectively. (C) siRNA-mediated knockdown does not lead to the nuclear access of p53. Huh6 cells were transiently transfected with siRNA against Parc or with the control siRNA. Twenty-four hours after transfection, cells were fractionated into cytoplasmic (C) and nuclear fractions (N), and subjected to Western blotting with the indicated antibodies.

acetylation. Unexpectedly, our present results revealed that Parc binds to p53 in Huh6 cells; however, the cytoplasmic retention of p53 in Huh6 cells is regulated in a Parc-independent manner. It is worth noting that the nicotinamide treatment of Huh6 cells leads to the inhibition of the oxidative stress-induced nuclear access of p53 as well as the pro-apoptotic activity of p53, indicating that the acetylation status of p53 plays an important role in the regulation of the cytoplasmic retention of p53.

It is well documented that p300/CBP-mediated acetylation of p53 at the COOH-terminal lysine residues including Lys-320, Lys-370, Lys-371, Lys-372, Lys-381 and Lys-382 enhances the transcriptional activity as well as stability of p53 (Brooks & Gu 2003). p300/CBP possess histone acetyl-transferase (HAT) activity (Ogryzko *et al.* 1996). Since the COOH-terminal lysine residues of p53 are tightly associated with the p300/CBP-mediated acetylation as well as the MDM2-mediated ubiquitination, it is possible that p53 acetylation catalyzed by p300/CBP reduces its ubiquitination levels by competition between acetylation and ubiquitination. Alternatively, Kawaguchi *et al.* (2006) described that the hyperacetylated forms of p53 are accumulated in cytoplasm. Histone deacetylases are divided into three classes including class I, II and III (de Ruijter *et al.* 2003). Among them, class III histone deacetylases are distinct from the remaining classes, and defined based on their similarity to the yeast silent information regulator 2 (Sir2). One of the human Sir2 homologues, SIRT2, was largely localized in cytoplasm of mammalian cultured cells, and its catalytic activity was significantly inhibited by nicotinamide (North *et al.* 2003). In addition, SIRT1, another member of the class III histone deacetylases, was sensitive to nicotinamide, and had an ability to deacetylate p53 at Lys-382 (Michishita *et al.* 2005). Although it remains unclear whether SIRT2 could deacetylate p53, it is likely that SIRT family member(s) might be involved in the regulation of the oxidative stress-induced nuclear translocation of p53 in Huh6 cells. However, the precise molecular mechanisms behind the cytoplasmic localization of p53 in HBL are still unknown.

According to our present findings, p53 was constitutively phosphorylated at Ser-15 and stabilized in cytoplasm of Huh6 cells. Accumulating evidence suggests that MDM2 binds to the NH_2-treminal region of p53, acts as an E3 ubiquitin protein ligase for p53 and thereby promotes its proteasome-dependent proteolytic degradation (Chen *et al.* 1993; Haupt *et al.* 1997; Honda *et al.* 1997; Kubbutat *et al.* 1997). Previous studies demonstrated that the DNA damage-induced phosphorylation of p53 at Ser-15 mediated by ATM, ATR and/or DNA-PK disrupts the

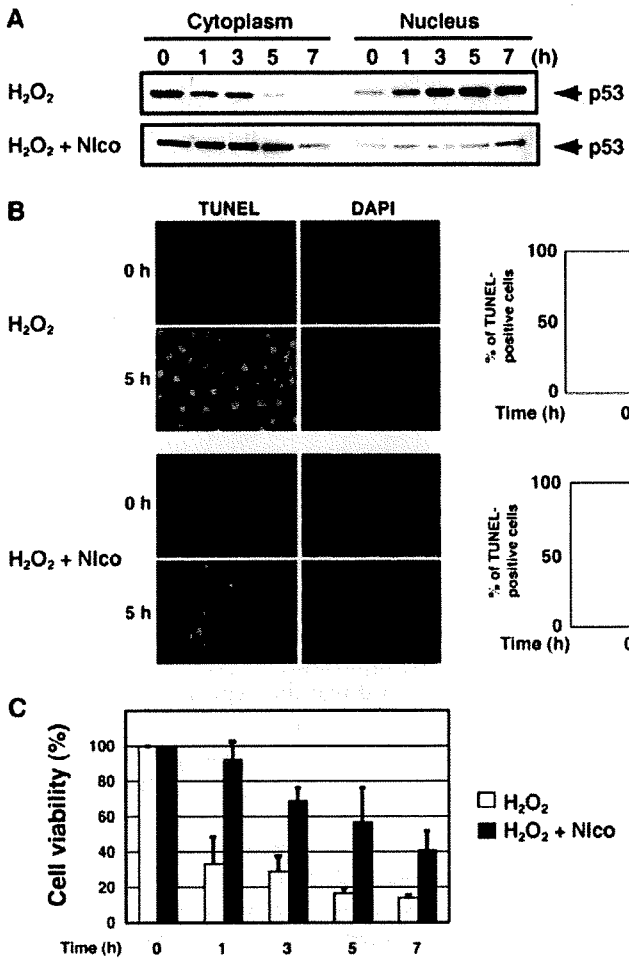

Figure 7 Deacetylase inhibitor nicotinamide inhibits the H_2O_2-mediated nuclear translocation of p53 and apoptotic cell death in Huh6 cells. (A) Huh6 cells were treated with H_2O_2 alone (1 mM) or with H_2O_2 (1 mM) plus nicotinamide (Nico, 5 mM). At the indicated time periods after the treatment with the drugs, cells were harvested and fractionated into cytoplasmic and nuclear fractions followed by Western blotting with the anti-p53 antibody. (B) TUNEL staining. Huh6 cells were exposed to the indicated combinations of the drug for 5 h. Apoptotic cells were identified by TUNEL assays. Cell nuclei were visualized by DAPI (left panels). The number of TUNEL-positive cells was scored, and expressed as a percentage of the total number of cells examined (right panels). H_2O_2-mediated apoptosis was significantly inhibited by nicotinamide. $P < 0.02$. (C) MTT cell survival assay. Huh6 cells were treated with the indicated combinations of the drug for 5 h or left untreated, and their viability was examined by MTT assays.

interaction between p53 and MDM2, resulting in the activation and stabilization of p53 (Shieh *et al.* 1997). Although the precise molecular mechanisms behind the constitutive phosphorylation of cytoplasmic p53 at Ser-15 remain unclear, it is likely that the significant accumulation of p53 in Huh6 cells without DNA damage might be due to the inhibition of the MDM2-mediated ubiquitination and proteasomal degradation of p53.

It has been shown that β-catenin, which is a key component of the Wnt signaling pathway, is frequently mutated or deleted in HBLs (Koch *et al.* 1999; Takayasu *et al.* 2001). These alterations occur in the NH_2-terminal region of β-catenin, which is responsible for the GSK3β-mediated phosphorylation (Aberle *et al.* 1997). Similar to the primary HBLs, HBL-derived Huh6 cells carry a mutant form of β-catenin at Thr-41 (Koch *et al.* 1999). GSK3β-mediated phosphorylation of β-catenin is required for its ubiquitin-dependent proteolytic degradation by 26S proteasome (Aberle *et al.* 1997). In accordance with this notion, a large amount of β-catenin was detectable in Huh6 cells in the absence of oxidative stress (data not shown). Intriguingly, it has been shown that DNA damage induces the nuclear accumulation of p53 as well as GSK3β, and p53 forms a stable complex with GSK3β (Watcharasit *et al.* 2002; Watcharasit *et al.* 2003). According to their results, p53 enhances the activity of GSK3β through the direct interaction with GSK3β in a phosphorylation-independent manner, and GSK3β activates the p53-dependent apoptotic pathway in response to DNA damage. Of note, we found that GSK3β was induced to be accumulated in cell nucleus in response to oxidative stress (data not shown). However, we have not yet explored the possible contribution of the functional interaction between p53 and GSK3β to the oxidative stress-induced apoptotic response in Huh6 cells.

Taken together, our present findings suggest that, in addition to β-catenin mutation, the abnormal cytoplasmic

localization of p53 might be involved in the genesis and development of HBL, and the acetylation status of p53 plays an important role in the cytoplasmic retention of p53. Furthermore, the oxidative stress-induced apoptotic cell death in Huh6 cells was strongly associated with the active nuclear translocation of p53, which was distinct from the CDDP-mediated nuclear accumulation of p53. Thus, our present results provide a novel targeted approach to enhance the HBL cell cytotoxity.

Experimental procedures

Cell culture

Human hepatoblastoma Huh6 cells and human hepatocellular carcinoma HepG2 cells were cultured in Dulbecco's modified Eagle's medium (DMEM) supplemented with 10% heat-inactivated fetal bovine serum (FBS; Invitrogen, Carlsbad, CA) and penicillin (100 IU/mL)/streptomycin (100 μg/mL). Cultures were maintained at 37 °C in a water-saturated atmosphere of 5% CO_2 in air.

RNA preparation and RT-PCR

Total RNA was extracted from cells exposed to cisplatin or hydrogen peroxide using the RNeasy Mini kit (Qiagen, Valencia, CA) according to the manufacturer's protocol. cDNA was reverse transcribed from 1 μg of total RNA with random primers and SuperScript II (Invitrogen) as recommended by the supplier. Following the reverse transcription, the resultant cDNA was subjected to the PCR-based amplification. For PCR analysis, oligonucleotide sequences used were as follows: *NOXA*, 5′-GCAAGAATGGAAGACCCTTG-3′ and 5′-GTGCTGAGTTGGCACTGAAA-3′; *Parc*, 5′-CGTCTCCTGAGCTTTGGTTC-3′ and 5′-CCTCATCTTCCTGCTCCAAG-3′; *GAPDH*, 5′-ACCTGACCTGCCGTCTAGAA-3′ and 5′-TCCACCACCCTGTTGCTGTA-3′. PCR products were resolved by 2% agarose gel electrophoresis, and visualized by ethidium bromide staining.

Western blot analysis

Cells were rinsed twice in ice-cold PBS and lyzed in SDS sample buffer containing 62.5 mM Tris–HCl, pH 6.8, 2% SDS, 2% β-mercaptoethanol and 0.01% bromophenol blue, followed by a brief sonication. After centrifugation at 10 000 *g* for 10 min at 4 °C, the supernatant was transferred to a new tube. The protein concentration was measured by the Bradford protein assay (Bio-Rad laboratories, Hercules, CA), using bovine serum albumin as a standard. For Western analysis, equal amounts of protein were separated by 10% SDS-PAGE, and electro-transferred on to Immobilon-P membranes (Millipore, Bedford, MA). The membranes were blocked overnight at 4 °C with TBS-T (50 mM Tris–HCl, pH 8.0, 100 mM NaCl and 0.1% Tween 20) containing 5% non-fat dry milk, and then incubated for 1 h at room temperature with the monoclonal anti-p53 (DO-1; Oncogene Research Products, Cambridge, MA), polyclonal anti-phosphorylated p53 at Ser-15 (Cell Signaling Technology, Beverly, MA), polyclonal anti-Parc (Calbiochem, La Jolla), or with polyclonal anti-actin antibody (20–33; Sigma Chemical Co., St. Louis, MO). After washing with TBS-T, the membranes were incubated with a horseradish peroxidase-conjugated appropriate secondary antibody (Jackson ImmunoResearch Laboratories, West Grove, PA) for 1 h at room temperature. The chemiluminescence reaction was performed using the ECL reagent (Amersham Biosciences, Piscataway, NJ).

Subcellular fractionation

Cells were washed twice in ice-cold PBS and lyzed in lysis buffer (10 mM Tris–HCl, pH 7.5, 1 mM EDTA, 0.5% NP-40) containing a protease inhibitor mix (Sigma Chemical Co.) for 10 min at 4 °C. Cell lysates were centrifuged at 10 000 *g* for 10 min at 4 °C to separate cytoplasmic fraction (supernatant). Insoluble materials were washed three times with the lysis buffer and nuclei were lyzed in 1× SDS sample buffer. The nuclear lysates were sonicated, centrifuged, and the supernatant was collected. The protein concentrations were determined by the Bradford protein assay (Bio-Rad Laboratories). The nuclear and cytoplasmic fractions were subjected to immunoblot analysis using the monoclonal anti-Lamin B (Ab-1; Oncogene Research Products) or monoclonal anti-α-tubulin antibody (Ab-2; NeoMarkers, Inc., Fremont, CA).

Indirect immunofluorescence

Huh6 cells on cover slips were fixed in ice-cold methanol for 5 min at room temperature and permeabilized with 0.2% Triton X-100 for 3 min at room temperature. After blocking with 3% bovine serum albumin in PBS, cover slips were incubated with anti-p53 antibody (DO-1) in PBS for 1 h at room temperature followed by incubation with rhodamine-conjugated secondary antibody (Invitrogen) in PBS for 1 h at room temperature. Cell nuclei were stained with DAPI.

Co-immunoprecipitation experiments

For co-immunoprecipitation experiments, cells were lyzed in lysis buffer (25 mM Tris–HCl, pH 8.0, 137 mM NaCl, 2.7 mM KCl, 1% Triton X-100) supplemented with protease inhibitor mixture for 30 min at 4 °C, and clarified by centrifugation at 10 000 *g* for 15 min at 4 °C. Equal amounts of whole cell lysates were precleared by incubation with 30 μL of 50% slurry of protein G-Sepharose beads (Amersham Biosciences). After brief centrifugation, the supernatants were collected and incubated with the normal mouse serum (NMS), or with monoclonal anti-p53 antibody (DO-1; Oncogene Research Products) at 4 °C for 2 h. The immune complexes were precipitated with the protein G-Sepharose beads for 1 h at 4 °C, and the nonspecific bound proteins were removed by washing the beads with the lysis buffer three times at 4 °C. Immunoprecipitated proteins were subjected to 10% SDS-PAGE, and Western blot analysis was carried out using the polyclonal anti-Parc antibody.

siRNA-mediated knockdown of p53

Huh6 cells were transfected with 2 μg of the empty plasmid (pSUPER; OligoEngine, Seattle, WA) or with pSUPER expression plasmid encoding siRNA against p53 (pSUPER-siRNA-p53) by using FuGENE 6 transfection reagent as recommended by the manufacturer (Roche Molecular Biochemicals, Mannheim, Germany). Forty-eight hours after transfection, the transfected cells were put under a selection pressure of 400 μg/mL of G418 (Sigma Chemical Co.). Thereafter, the selection medium was replaced every 3 days. Two weeks after the selection in G418, drug-resistant clones were isolated and allow to proliferate in medium containing G418 (400 μg/mL).

Cell survival assay

Cell viability was determined by MTT assay and expressed as percent viable cells. In brief, Huh6 or HepG2 cells were seeded in 96-well microtiter plates (5×10^3 cells/well) with 100 μL of complete medium. The next day, the medium was changed and cells were exposed to the indicated concentrations of hydrogen peroxide. At the indicated time periods after the treatment with hydrogen peroxide, 10 μL of MTT labeling reagent were added to each well, and the cultures were incubated for 1 h at 37 °C. The absorbance readings for each well were carried out at a wavelength of 570 nm using the microplate reader (model 450; Bio-Rad Laboratories).

Apoptotic analysis

Apoptotic cells were detected by *In Site* Cell Death Detection Kit, TMR red (Roche Molecular Biochemicals). In brief, Huh6 cells were grown overnight on glass cover slips at 37 °C. Five hours after the treatment with hydrogen peroxide, cells were washed in PBS, fixed in 4% paraformaldehyde for 1 h at room temperature and then permeabilized with 0.1% Triton X-100 for 2 min on ice. The cells were subsequently incubated with TUNEL reaction mixture for 1 h at 37 °C in a humidified atmosphere in the dark. The cover slips were mounted onto microscope slides using the VECTASHIELD containing DAPI (Vector Laboratories, Burlingame, CA), and examined under a Fluoview laser scanning confocal microscope (Olympus, Tokyo, Japan).

Tumor tissues and immunohistochemistry

Hepatoblastoma tissues, which were collected at Gunma Children's Medical Center, were obtained at surgery, immediately frozen and stored at −80 °C until use. Sections from formalin-fixed, paraffin-embedded tumor samples were cut at 4-μm thickness and subjected to immunostaining. In brief, antigen retrieval was achieved by the treatment of deparaffinized sections with microwaves in 0.1 M citrate buffer (pH 6.0) for 20 min, followed by cooling at room temperature prior to incubation with the primary antibody. Tissue sections were incubated with monoclonal anti-p53 antibody (PAb240; Calbiochem) overnight at 4 °C and washed in PBS. The bound antibody was detected using the strepto-avidin-biotin complex method (Nichirei Corp., Tokyo, Japan) and visualized by diaminobenzidine tetrahydrochloride.

Acknowledgements

We are grateful to Dr M. Kuroiwa for kindly providing the hepatoblastoma tissues and Ms Y. Nakamura for assistance with DNA sequencing. This work was supported in part by a Grant-in-Aid from the Ministry of Health, Labour and Welfare for Third Term Comprehensive Control Research for Cancer, a Grant-in-Aid for Scientific Research on Priority Areas from the Ministry of Education, Culture, Sports, Science and Technology of Japan, a Grant-in-Aid for Scientific Research from Japan Society for the Promotion of Science, and a Grant from Uehara Memorial Foundation.

References

Aberle, H., Bauer, A., Stappert, J., Kispert, A. & Kemler, R. (1997) β-catenin is a target for the ubiquitin-proteasome pathway. *EMBO J.* **16**, 3797–3804.

Aden, D.P., Fogel, A., Plotkin, S., Damjanov, I. & Knowles, B.B. (1979) Controlled synthesis of HBsAg in a differentiated human liver carcinoma-derived cell line. *Nature* **282**, 615–616.

Bosari, S., Viale, G., Roncalli, M., Graziani, D., Borsani, G., Lee, A.K. & Coggi, G. (1995) p53 gene mutations, p53 protein accumulation and compartmentalization in colorectal adenocarcinoma. *Am. J. Pathol.* **147**, 790–798.

Bressac, B., Galvin, K.M., Liang, J., Isselbacher, K.J., Wands, J.R. & Ozturk, M. (1990) Abnormal structure and expression of p53 gene in human hepatocellular carcinoma. *Proc. Natl. Acad. Sci. USA* **87**, 1973–1977.

Brooks, C.L. & Gu, W. (2003) Ubiquitination, phosphorylation and acetylation: the molecular basis for p53 regulation. *Curr. Opin. Cell Biol.* **15**, 164–171.

Chen, T.C., Hsieh, L.L. & Kuo, T.T. (1995) Absence of p53 gene mutation and infrequent overexpression of p53 protein in hepatoblastoma. *J. Pathol.* **176**, 243–247.

Chen, J., Marechal, V. & Levine, A.J. (1993) Mapping of the p53 and mdm-2 interaction domains. *Mol. Cell. Biol.* **13**, 4107–4114.

Doi, I. (1976) Establishment of a cell line and its clonal sublines from a patient with hepatoblastoma. *Gann* **67**, 1–10.

Dornan, D., Wertz, I., Shimizu, H., Arnott, D., Frantz, G.D., Dowd, P., O'Rourke, K., Koeppen, H. & Dixit, V.M. (2004) The ubiquitin ligase COP1 is a critical negative regulator of p53. *Nature* **429**, 86–92.

Fritsche, M., Haessler, C. & Brandner, G. (1993) Induction of nuclear accumulation of the tumor-suppressor protein p53 by DNA-damaging agents. *Oncogene* **8**, 307–318.

Gu, W. & Roeder, R.G. (1997) Activation of p53 sequence-specific DNA binding by acetylation of the p53 C-terminal domain. *Cell* **90**, 595–606.

Harada, N., Miyoshi, H., Murai, N., Oshima, H., Tamai, Y., Oshima, M. & Taketo, M.M. (2002) Lack of tumorigenesis in the mouse liver after adenovirus-mediated expression of a dominant stable mutant of β-catenin. *Cancer Res.* **62**, 1971–1977.

Harada, N., Oshima, H., Katoh, M., Tamai, Y., Oshima, M. & Taketo, M.M. (2004) Hepatocarcinogenesis in mice with β-catenin and Ha-ras gene mutations. *Cancer Res.* **64**, 48–54.

Haupt, Y., Maya, R., Kazaz, A. & Oren, M. (1997) Mdm2 promotes the rapid degradation of p53. *Nature* **387**, 296–299.

Henderson, B.R. & Fagotto, F. (2002) The ins and outs of APC and β-catenin nuclear transport. *EMBO Rep.* **3**, 834–839.

Hollstein, M., Sidransky, D., Vogelstein, B. & Harris, C.C. (1991) p53 mutations in human cancers. *Science* **253**, 49–53.

Honda, R., Tanaka, H. & Yasuda, H. (1997) Oncoprotein MDM2 is a ubiquitin ligase E3 for tumor suppressor p53. *FEBS Lett.* **420**, 25–27.

Hsu, I.C., Tokiwa, T., Bennett, W., Metcalf, R.A., Welsh, J.A., Sun, T. & Harris, C.C. (1993) p53 gene mutation and integrated hepatitis B viral DNA sequences in human liver cancer cell lines. *Carcinogenesis* **14**, 987–992.

Hughes, L.J. & Michels, V.V. (1992) Risk of hepatoblastoma in familial adenomatous polyposis. *Am. J. Med. Genet.* **43**, 1023–1025.

Kawaguchi, Y., Ito, A., Appella, E. & Yao, T.P. (2006) Charge modification at multiple C-terminal lysine residues regulates p53 oligomerization and its nucleus-cytoplasm trafficking. *J. Biol. Chem.* **281**, 1394–1400.

Koch, A., Denkhaus, D., Albrecht, S., Leuschner, I., von Schweinitz, D. & Pietsch, T. (1999) Childhood hepatoblastomas frequently carry a mutated degradation targeting box of the β-catenin gene. *Cancer Res.* **59**, 269–273.

Kubbutat, M.H., Jones, S.N. & Vousden, K.H. (1997) Regulation of p53 stability by Mdm2. *Nature* **387**, 299–303.

Kusafuka, T., Fukuzawa, M., Oue, T., Komoto, Y., Yoneda, A. & Okada, A. (1997) Mutation analysis of p53 gene in childhood malignant solid tumors. *J. Pediatr. Surg.* **32**, 1175–1180.

Leng, R.P., Lin, Y., Ma, W., Wu, H., Lemmers, B., Chung, S., Parant, J.M., Lozano, G., Hakem, R. & Benchimol, S. (2003) Pirh2, a p53-induced ubiquitin-protein ligase, promotes p53 degradation. *Cell* **112**, 779–791.

Llovet, J.M., Burroughs, A. & Bruix, J. (2003) Hepatocellular carcinoma. *Lancet* **362**, 1907–1917.

Lluis, J.M., Morales, A., Biasco, C., Colell, A., Mari, M., Garcia-Ruiz, C. & Fernandez-Checa, J.C. (2005) Critical role of mitochondrial glutathione in the survival of hepatocytes during hypoxia. *J. Biol. Chem.* **280**, 3224–3232.

Michishita, E., Park, J.Y., Burneskis, J.M., Barrett, J.C. & Horikawa, I. (2005) Evolutionarily conserved and nonconserved cellular localizations and functions of human SIRT proteins. *Mol. Biol. Cell* **16**, 4623–4635.

Moll, U.M., LaQuaglia, M., Benard, J. & Riou, G. (1995) Wild-type p53 protein undergoes cytoplasmic sequestration in undifferentiated neuroblastomas but not in differentiated tumors. *Proc. Natl. Acad. Sci. USA* **92**, 4407–4411.

Moll, U.M., Riou, G. & Levine, A.J. (1992) Two distinct mechanisms alter p53 in breast cancer: mutation and nuclear exclusion. *Proc. Natl. Acad. Sci. USA* **89**, 7262–7266.

Nagase, H. & Nakamura, Y. (1993) Mutations of the APC (adenomatous polyposis coli) gene. *Hum. Mutat.* **2**, 425–434.

Nikolaev, A.Y., Li, M., Puskas, N., Qin, J. & Gu, W. (2003) Parc: a cytoplasmic anchor for p53. *Cell* **112**, 29–40.

North, B.J., Marshall, B.L., Borra, M.T., Denu, J.M. & Verdin, E. (2003) The human Sir2 ortholog, SIRT2, is an NAD^+-dependent tubulin deacetylase. *Mol. Cell* **11**, 437–444.

Ogryzko, V.V., Schiltz, R.L., Russanova, V., Howard, B.H. & Nakatani, Y. (1996) The transcriptional coactivators p300 and CBP are histone acetyltransferases. *Cell* **29**, 953–959.

Ohnishi, H., Kawamura, M., Hanada, R., Kaneko, Y., Tsunoda, Y., Hongo, T., Bessho, F., Yokomori, K. & Hayashi, Y. (1996) Infrequent mutations of the TP53 gene and no amplification of the MDM2 gene in hepatoblastomas. *Genes Chromosomes Cancer* **15**, 187–190.

Ostermeyer, A.G., Runko, E., Winkfield, B., Ahn, B. & Moll, U.M. (1996) Cytoplasmically sequestered wild-type p53 protein in neuroblastoma is relocated to the nucleus by a C-terminal peptide. *Proc. Natl. Acad. Sci. USA* **93**, 15190–15194.

Prives, C. & Hall, P.A. (1999) The p53 pathway. *J. Pathol.* **187**, 112–126.

de Ruijter, A.J., van Gennip, A.H., Caron, H.N., Kemp, S. & van Kuilenburg, A.B. (2003) Histone deacetylases (HDACs): characterization of the classical HDAC family. *Biochem. J.* **370**, 737–749.

Shieh, S.Y., Ikeda, M., Taya, Y. & Prives, C. (1997) DNA damage-induced phosphorylation of p53 alleviates inhibition by MDM2. *Cell* **91**, 325–334.

Sionov, R.V. & Haupt, Y. (1999) The cellular response to p53: the decision between life and death. *Oncogene* **18**, 6145–6157.

Stommel, J.M., Marchenko, N.D., Jimenez, G.S., Moll, U.M., Hope, T.J. & Wahl, G.M. (1999) A leucine-rich nuclear export signal in the p53 tetramerization domain: regulation of subcellular localization and p53 activity by NES masking. *EMBO J.* **18**, 1660–1672.

Takayasu, H., Horie, H., Hiyama, E., Matsunaga, T., Hayashi, Y., Watanabe, Y., Suita, S., Kaneko, M., Sasaki, F., Hashizume, K., Ozaki, T., Furuuchi, K., Tada, M., Ohnuma, N. & Nakagawara, A. (2001) Frequent deletions and mutations of the β-catenin gene are associated with overexpression of cyclin D1 and fibronectin and poorly differentiated histology in childhood hepatoblastoma. *Clin. Cancer Res.* **7**, 901–908.

Vogan, K., Berstein, M., Leclerc, J.M., Brisson, L., Brossard, J., Brodeur, G.M., Pelletier, J. & Gros, P. (1993) Absence of p53 gene mutations in primary neuroblastomas. *Cancer Res.* **53**, 5269–5273.

Vogelstein, B., Lane, D. & Levine, A.J. (2000) Surfing the p53 network. *Nature* **408**, 307–310.

Vousden, K.H. & Lu, X. (2002) Live or let die: the cell's response to p53. *Nat. Rev. Cancer* **2**, 594–604.

Watcharasit, P., Bijur, G.N., Song, L., Zhu, J., Chen, X. & Jope, R.S. (2003) Glycogen synthase kinase-3β (GSK3β) binds to and promotes the actions of p53. *J. Biol. Chem.* **278**, 48872–48879.

Watcharasit, P., Bijur, G.N., Zmijewski, J.W., Song, L., Zmijewska, A., Chen, X., Johnson, G.V. & Jope, R.S. (2002) Direct, activating interaction between glycogen synthase kinase-3β and p53 after DNA damage. *Proc. Natl. Acad. Sci. USA* **99**, 7951–7955.

Received: 20 October 2006
Accepted: 21 December 2006

Available online at www.sciencedirect.com
ScienceDirect
Biochemical and Biophysical Research Communications 354 (2007) 892–898
BBRC
www.elsevier.com/locate/ybbrc

Functional characterization of a new p53 mutant generated by homozygous deletion in a neuroblastoma cell line

Yohko Nakamura [1], Toshinori Ozaki [1], Hidetaka Niizuma, Miki Ohira, Takehiko Kamijo, Akira Nakagawara *

Division of Biochemistry, Chiba Cancer Center Research Institute, Chiba 260-8717, Japan

Received 11 January 2007
Available online 22 January 2007

Abstract

p53 is a key modulator of a variety of cellular stresses. In human neuroblastomas, p53 is rarely mutated and aberrantly expressed in cytoplasm. In this study, we have identified a novel p53 mutant lacking its COOH-terminal region in neuroblastoma SK-N-AS cells. p53 accumulated in response to cisplatin (CDDP) and thereby promoting apoptosis in neuroblastoma SH-SY5Y cells bearing wild-type *p53*, whereas SK-N-AS cells did not undergo apoptosis. We found another p53 (p53ΔC) lacking a part of oligomerization domain and nuclear localization signals in SK-N-AS cells. p53ΔC was expressed largely in cytoplasm and lost the transactivation function. Furthermore, a 3′-part of the *p53* locus was homozygously deleted in SK-N-AS cells. Thus, our present findings suggest that p53 plays an important role in the DNA-damage response in certain neuroblastoma cells and it seems to be important to search for *p53* mutations outside DNA-binding domain.

Keywords: Apoptosis; Cisplatin; Homozygous deletion; Neuroblastoma; p53

p53 plays a pivotal role in the regulation of cell cycle arrest and apoptosis. *p53* is one of the most frequently mutated genes in human tumors [1,2] and *p53*-deficient mice developed spontaneous tumors [3]. Upon a variety of cellular stresses, p53 accumulates in nucleus through post-translational modifications including phosphorylation and acetylation and thereby exerting its function [4]. Pro-apoptotic function of p53 is closely linked to its DNA-binding activity. p53 acts as a transcription factor to transactivate a variety of its target genes. Indeed, 95% of *p53* mutations in human tumors occur within its DNA-binding region and these mutations inactivate pro-apoptotic function of p53 [4].

Alternatively, p53 is inhibited by various mechanisms. MDM2 acts as an E3 ubiquitin ligase for p53 and promotes its proteolytic degradation through ubiquitin–proteasome pathway [5,6]. Subcellular distribution of p53 also plays a key role in the regulation of p53 [4]. p53 contains three nuclear localization signals (NLS I, II, and III) in its COOH-terminal region [7,8]. In contrast to other human tumors, *p53* is rarely mutated in neuroblastomas [9]. Neuroblastoma cells showed a cytoplasmic localization of wild-type p53 and exhibited an impaired p53-mediated cell cycle arrest in response to DNA damage, suggesting that there exists a mutation-independent mechanism of p53 inactivation [10–12]. Intriguingly, Nikolaev et al. demonstrated that Parkin-like ubiquitin ligase termed Parc serves as an anchor protein that tethers p53 in cytoplasm and thereby regulating subcellular localization and function of p53 [13].

In this study, we have identified a novel p53 mutant (p53ΔC) homozygously deleted in neuroblastoma SK-N-AS cells and our current studies suggest that *p53* status plays an important role in the cell fate determination of certain neuroblastoma cells in response to DNA damage.

* Corresponding author. Fax: +81 43 265 4459.
E-mail address: akiranak@chiba-cc.jp (A. Nakagawara).
[1] These authors contributed equally to this work.

0006-291X/$ - see front matter © 2007 Elsevier Inc. All rights reserved.
doi:10.1016/j.bbrc.2007.01.057

Materials and methods

Cell culture and transfection. Neuroblastoma cells were grown in RPMI 1640 medium supplemented with 10% heat-inactivated fetal bovine serum (FBS, Invitrogen) and antibiotic mixture in a humidified atmosphere of 5% CO_2 in air at 37 °C. For transfection, cells were transfected with the indicated expression plasmids using LipofectAMINE 2000 according to the manufacturer's instructions (Invitrogen).

Construction of p53 mutant. cDNA encoding p53 mutant was amplified by PCR using cDNA from SK-N-AS cells. Forward and reverse primers were 5′-AATATTTCACCCTTCAGGTACTAAG-3′ (forward) and 5′-CTCGAGTCACTGCCCCCTGATGGC-3′ (reverse). *Ssp*I and *Xho*I sites shown in boldface type were introduced into forward and reverse primers, respectively. PCR products were gel-purified and subcloned into pGEM-T plasmid (Promega). Constructs were confirmed by sequencing and then digested with *Ssp*I and *Xho*I. The digested fragment was again gel-purified and then ligated with the *Ssp*I and *Bam*HI fragment of FLAG-p53 to give pcDNA3-FLAG-p53CΔ.

RNA preparation and RT-PCR analysis. Total RNA was prepared using RNeasy Mini kit (Qiagen) following the manufacturer's protocol. cDNA was synthesized using SuperScript II with random primers (Invitrogen) and amplified by PCR using primers as described: *p53*: forward, 5′-CTGCCCTCAACAAGATGTTTTG-3′, and reverse, 5′-CTATCTGAGCAGCGCTCATGG-3′; *p21*^{WAF1}: forward, 5′-ATGAAATTCACCCCCTTTCC-3′, and reverse, 5′-CCCTAGGCTGTGCTCACTTC-3′; *Bax*: forward, 5′-TTTGCTTCAGGGTTTCATCC-3′, and reverse, 5′-CAGTTGAAGTTGCCGTCAGA-3′; *p53AIP1*: forward, 5′-CCAAGTTCTCTGCTTTC-3′ and reverse, 5′-AGCTGAGCTCAAATGCTGAC-3′; *PUMA*: forward, 5′-TATGGATCCCGCACCATGGACTACAAGGACGACGATGACAAGGCCCGCGCACGCCAG-3′ and reverse, 5′-TATGGATCCCTACATGGTGCAGAGAAAGTCCCCC-3′; and *GAPDH*: forward, 5′-ACCTGACCTGCCGTCTAGAA-3′, and reverse, 5′-TCCACCACCCTGTTGCTGTA-3′.

Southern blotting. Genomic DNA was digested with *Pst*I, separated by 1% agarose gel electrophoresis, and transferred onto nylon membranes. Hybridization was performed at 65 °C in a solution containing 1 M NaCl, 1% *N*-lauroyl sarcosine, 7.5% dextran sulfate, 100 μg of heat-denatured salmon sperm DNA/ml, and radio-labeled DNA. After hybridization, membranes were washed twice with 2× SSC/0.1% *N*-lauroyl sarcosine at 50 °C and exposed to an X-ray film at −70 °C.

Immunoblotting. Cells were lysed in lysis buffer containing 25 mM Tris–HCl, pH 8.0, 137 mM NaCl, 2.7 mM KCl, 1% Triton X-100, and protease inhibitor mixture (Sigma). Lysates were separated by SDS–PAGE and transferred onto Immobilon-P membranes (Millipore). Membranes were probed with anti-p53 (DO-1, Calbiochem), anti-p53 (PAb122, BD Pharmingen), anti-phosphorylated p53 at Ser-15 (Cell Signaling) or with anti-actin (20–33, Sigma) followed by incubation with HRP-conjugated goat anti-mouse or anti-rabbit IgG secondary antibody (Cell Signaling). Immunoreactive bands were detected using chemiluminescence (ECL, Amersham Biosciences).

Subcellular fractionation. Cells were lysed in lysis buffer containing 10 mM Tris–HCl, pH 7.5, 1 mM EDTA, 0.5% NP-40, and protease inhibitor mixture (Sigma). Lysates were centrifuged to separate soluble (cytosolic) from insoluble (nuclear) fractions. The nuclear and cytosolic fractions were subjected to immunoblotting using anti-p53, anti-Lamin B (Ab-1, Oncogene Research products) or with anti-tubulin-α (Ab-2, NeoMarkers).

Array-based comparative genomic hybridization (CGH) analysis. Whole genome arrays of 2464 bacterial artificial chromosome (BAC) clones were hybridized simultaneously with 500 ng of target DNA (SK-N-AS, RTBM1, and SH-SY5Y) and reference DNA (normal female genomic DNA). Target DNAs were labeled with Cy3-dCTP and reference DNAs with Cy5-dCTP by random priming. Hybridization, scanning, and data processing were conducted as described previously [14,15].

Cell survival assays. Cells were plated at a density of 5000 cells/well in 96-well tissue culture plates. After attachment overnight, medium was replaced and treated with CDDP for 24 h. Cell viability was measured by MTT assay.

Flow cytometry. Floating and adherent cells were pooled and fixed in ice-cold 70% ethanol for 4 h at −20 °C. Cells were then stained with 10 mg/ml of PI (Sigma) in the presence of 250 mg/ml of RNase A at 37 °C for 30 min in the dark. Number of cells with sub-G1 DNA content was measured by flow cytometry (FACScan, Becton–Dickinson).

TUNEL assay. Apoptotic cells were identified using an *in situ* cell detection, peroxidase kit (Roche Applied Science). Briefly, cells were fixed in 4% paraformaldehyde and permeabilized with 0.1% Triton X-100. The labeling reaction was performed using TMR red-labeled dUTP together with other nucleotides by terminal deoxynucleotidyl transferase for 1 h in the dark at 37 °C. Then, cells were mounted and the incorporated TMR red-labeled dUTP was analyzed using a Fluoview laser scanning confocal microscope (Olympus).

Luciferase reporter assay. H1299 cells were co-transfected with pcDNA3, FLAG-p53 or FLAG-p53ΔC expression plasmid, p53-responsive luciferase reporter (*p21*^{WAF1}, *MDM2* or *Bax*), and pRL-TK *Renilla* luciferase cDNA. Forty-eight hours after transfection, firefly and *Renilla* luciferase activities were measured with dual-luciferase reporter assay system according to the manufacturer's instructions (Promega).

Colony formation assay. Forty-eight hours after transfection, SK-N-AS cells were transferred to fresh medium containing G418 (400 μg/ml). After 16 days of selection, drug-resistant colonies were fixed in methanol and stained with Giemsa's solution.

Results

DNA-damage response in human neuroblastoma cells

To determine the effects of genotoxic agents on neuroblastomas, human neuroblastoma SH-SY5Y and SK-N-AS cells were exposed to cisplatin (CDDP) and their viabilities were examined by MTT assays. As shown in Fig. 1A, their viabilities were significantly decreased in response to CDDP. To address whether CDDP could induce apoptosis, we performed TUNEL assay. As shown in Fig. 1B, we observed a higher number of TUNEL-positive SH-SY5Y cells exposed to CDDP, whereas CDDP had undetectable effects on SK-N-AS cells. We further determined apoptotic cells as sub-G1 population by flow cytometry. As seen in Fig. 1C, a significant increase in number of SH-SY5Y cells with sub-G1 DNA content was observed after CDDP treatment, whereas CDDP treatment of SK-N-AS cells resulted in an increase in S-phase cells but not in G2/M-phase cells. Consistent with these results, *thymidine kinase* (S-phase marker) [16] was increased in CDDP-treated SK-N-AS cells, whereas *Plk1* (M-phase marker) [17] remained unchanged regardless of CDDP treatment (data not shown).

We then examined whether p53-dependent apoptotic pathway could be activated in response to CDDP. As shown in Fig. 1D, p53 was phosphorylated at Ser-15 in SH-SY5Y cells exposed to CDDP. *p53* remained unchanged regardless of CDDP treatment, whereas p53 target genes including *p21*^{WAF1}, *Bax*, and *PUMA* were transactivated in response to CDDP. In contrast, CDDP-mediated phosphorylation of p53 at Ser-15 was undetectable in SK-N-AS cells. *p21*^{WAF1} was induced in response to CDDP, however, CDDP-mediated up-regulation of pro-apoptotic *Bax* and *PUMA* was undetectable, suggesting that p53 pro-apoptotic function might be lost in SK-N-AS cells.

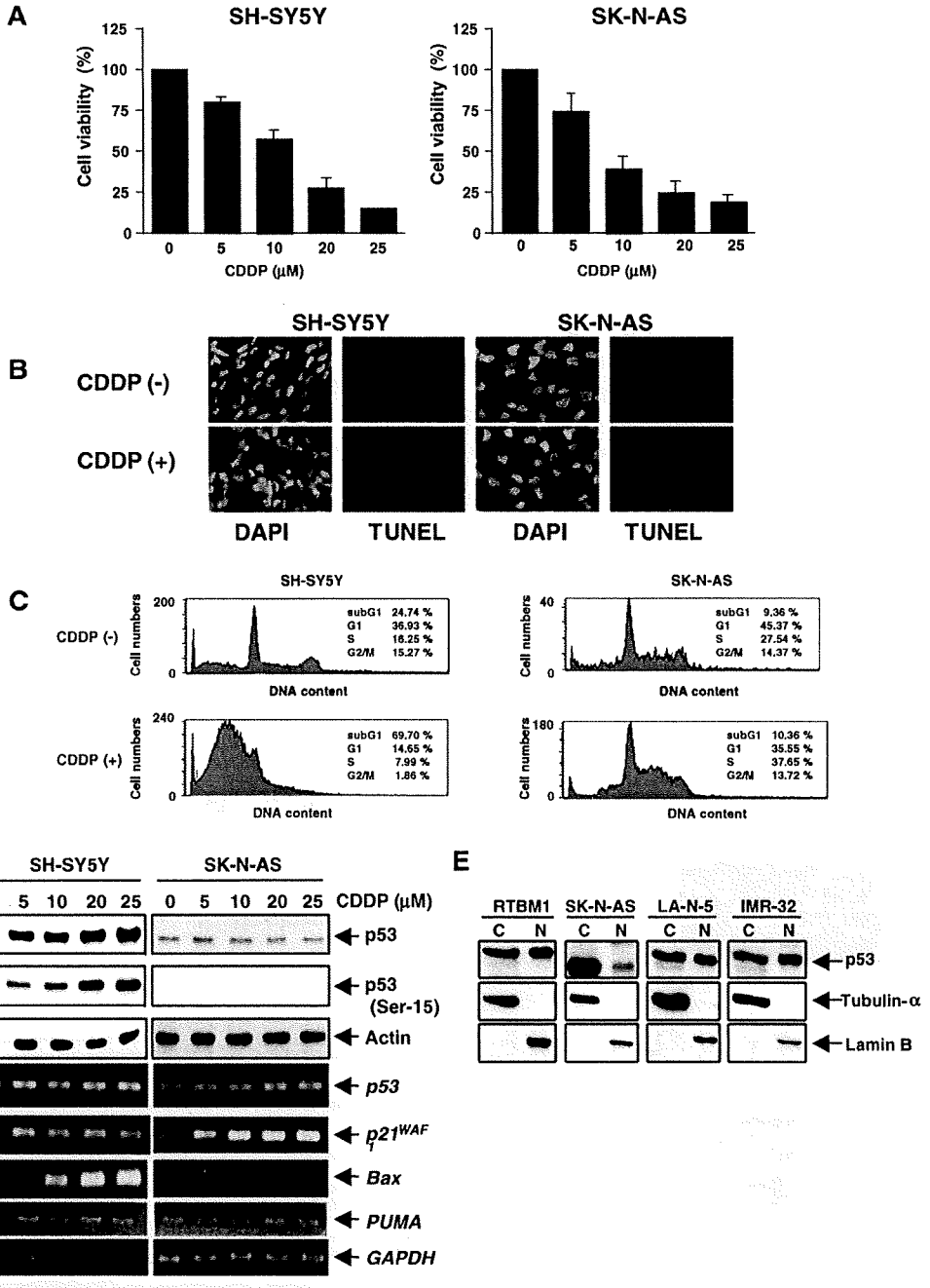

Fig. 1. Differential effects of CDDP on neuroblastoma cells. (A) Cell survival assays. Twenty-four hours after CDDP treatment, cell viability was analyzed by MTT assays. (B) TUNEL staining. Twenty-four hours after CDDP treatment (20 μM), apoptotic cells were detected by TUNEL staining. Cell nuclei were stained with DAPI. (C) FACS analysis. SH-SY5Y and SK-N-AS cells were treated as in (B). Twenty-four hours after CDDP treatment, cell cycle distributions were analyzed by FACS. Shown are the representatives of three independent experiments. (D) CDDP-induced accumulation of p53 in neuroblastoma cells. Twenty-four hours after CDDP treatment, lysates and total RNA were subjected to immunoblotting (upper panels) and RT-PCR (lower panels), respectively. For protein loading control, actin levels were checked by immunoblotting. For RT-PCR, *GAPDH* was used as a loading control. (E) Subcellular localization of p53. The indicated neuroblastoma cells were fractionated into cytoplasmic (C) and nuclear (N) fractions and subcellular distribution of p53 was analyzed by immunoblotting. Tubulin-α and Lamin B were used as cytoplasmic and nuclear markers, respectively.

To investigate molecular mechanism(s) behind p53 dysfunction in SK-N-AS cells, we examined subcellular localization of p53 in various neuroblastoma cells. As shown in Fig. 1E, p53 was detected in cytoplasm and nucleus of RTBM1, LA-N-5, and IMR-32 cells bearing wild-type *p53* (data not shown). Of note, p53 was abundantly expressed in cytoplasm of SK-N-AS cells and its molecular mass was smaller than those of other

cells, indicating that it might be due to certain structural aberrations.

Structural aberration of p53 in SK-N-AS cells

To address whether p53 could have any aberrations in SK-N-AS cells, we amplified the indicated genomic regions of *p53* using genomic DNA from SK-N-AS cells. RTBM1 cells were used as a positive control. As shown in Fig. 2A, PCR-based amplification using primer sets including P1, P2, P6, and P7 successfully generated estimated sizes of PCR products, whereas remaining primer sets (P3–P5) did not, suggesting that the genomic region containing exons 10 and 11 of *p53* might be lost in SK-N-AS cells.

To confirm genomic aberrations within *p53* locus in SK-N-AS cells, we performed Southern analysis. Radio-labeled *p53* cDNA probe failed to detect *Pst*I fragment (2.0 kb in length) which contains exons 10 and 11 in SK-N-AS cells (Fig. 2B). Our array-based comparative genomic hybridization (CGH) analysis demonstrated that there exists a large range of allelic deletion of chromosome 17p where *p53* is located in SK-N-AS cells (Fig. 2C). Furthermore, anti-p53 antibody which recognizes p53 extreme COOH-terminal portion could not detect p53 in SK-N-AS cells (Fig. 2D). Collectively, our results suggest that p53 COOH-terminal region is homozygously deleted in SK-N-AS cells. We then cloned *p53* cDNA. As shown in Fig. 2E, a newly identified p53 (p53ΔC) was composed of 369 amino acids including unique COOH-terminal structure (estimated molecular mass of 49 kDa), lacked a part of oligomerization domain, and completely lost NLS II and III. The 3′-side of intron 9 and the downstream region containing exons 10 and 11 were deleted in SK-N-AS cells. Its unique COOH-terminal amino acids were derived from intron 9, suggesting that accurate splicing event might be abrogated and thereby generating p53ΔC.

Dysfunction of p53ΔC

To ask whether p53ΔC could have functional differences as compared with wild-type p53, FLAG-p53 or FLAG-p53ΔC was expressed in SK-N-AS cells and their subcellular localization was examined. As shown in Fig. 3A, FLAG-p53 was detectable in cytoplasm and nucleus,

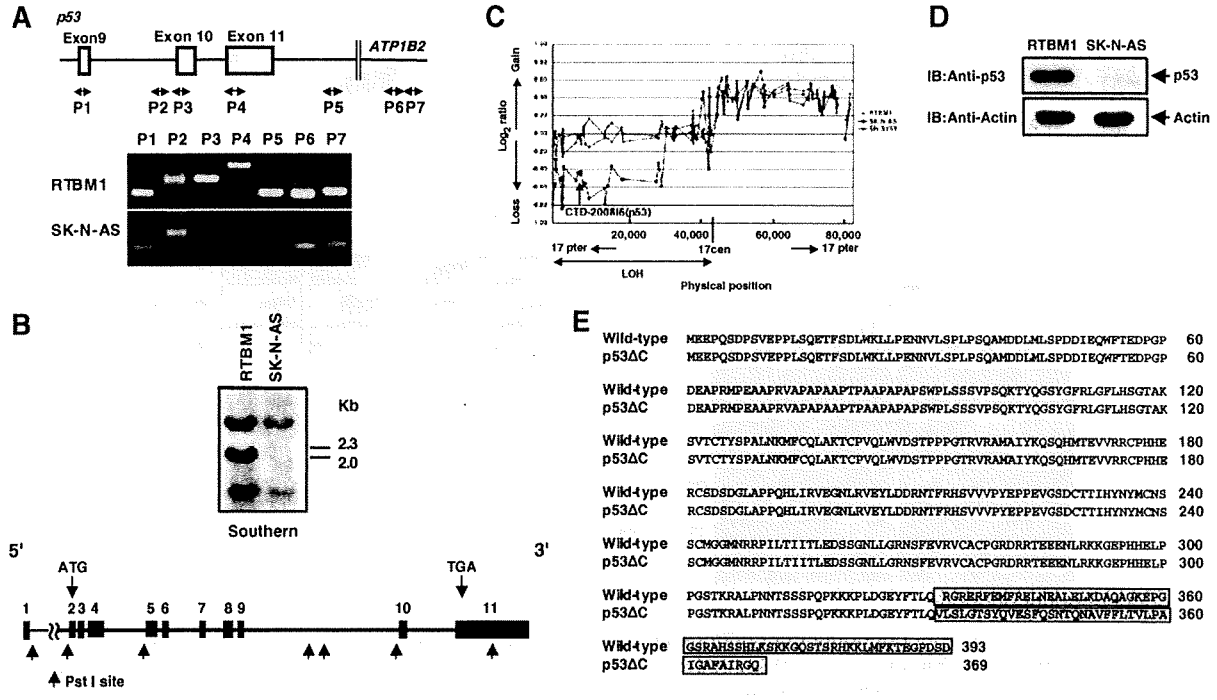

Fig. 2. p53 COOH-terminal region is deleted in SK-N-AS cells. (A) Genomic structure of human *p53* locus and positions of PCR primers (P1–P7) are shown. *ATP1B2* encodes ATPase, Na^+/K^+ transporting β2 (upper panel). Genomic DNA from RTBM1 and SK-N-AS cells was subjected to PCR using the indicated primers (lower panels). (B) Southern blot analysis. Genomic DNA was digested with *Pst*I, separated by 1% agarose gel, transferred onto nylon membrane, and probed with the radio-labeled *p53* cDNA. Schematic diagram of human *p53* and positions of *Pst*I sites are also shown. (C) Array-based comparative genomic hybridization (CGH) analysis. Hybridization was performed as described under Materials and methods. Arrays were scanned and images processed using custom software. We normalized relative ratios of tumor and normal signals by setting the value of the median relative ratio equal to 1. The data were then transformed into log 2 space and plotted as a histogram to determine cutoffs for scoring loss or gain. Three Gaussian distribution curves were fitted to the histogram, and values >3 SD from the central Gaussian were scored as losses or gains for that tumor. (D) Immunoblotting. Lysates from RTBM1 and SK-N-AS were processed for immunoblotting with the specific antibody against p53 extreme COOH-terminal portion. (E) Amino acid sequence alignment of wild-type p53 and p53ΔC. The different amino acid residues between them are boxed.

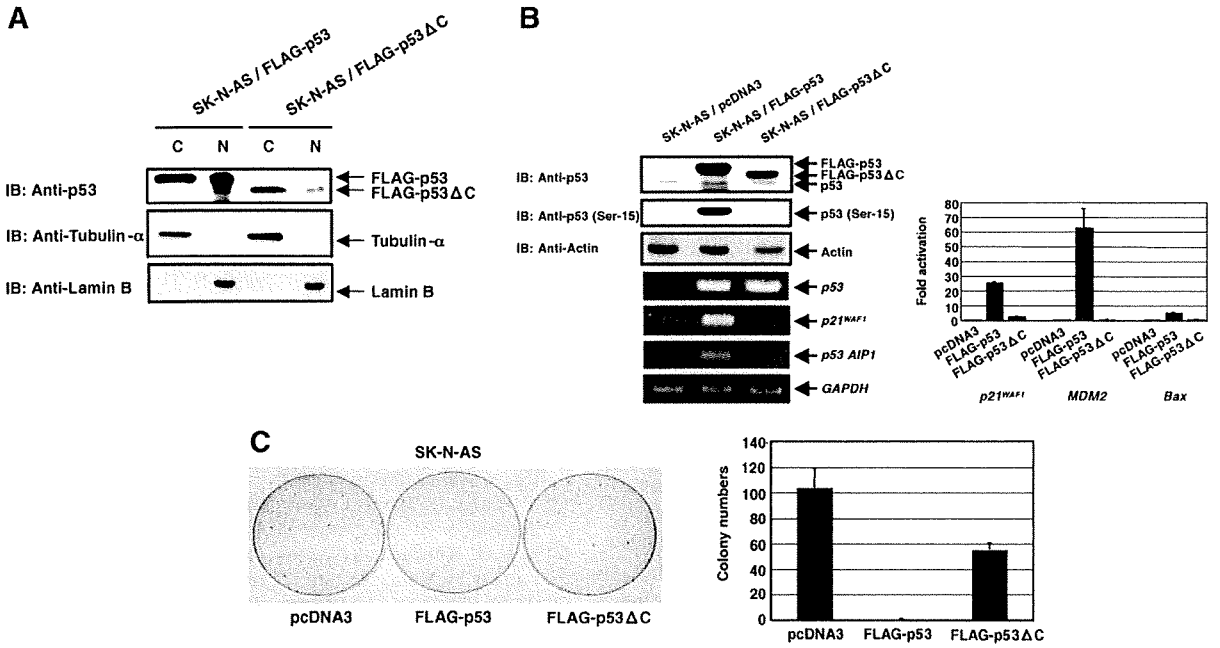

Fig. 3. Loss of function of p53ΔC. (A) Subcellular localization of exogenously expressed wild-type p53 and p53ΔC. SK-N-AS cells were transfected with the indicated expression plasmids. Forty-eight hours after transfection, cells were fractionated into cytoplasmic (C) and nuclear (N) fractions followed by immunoblotting with anti-p53 antibody. (B) Possible effects of COOH-terminal deletion of p53 on its transcriptional activity. SK-N-AS cells were transfected with the indicated expression plasmids. Forty-eight hours after transfection, lysates and total RNA were subjected to immunoblotting and RT-PCR, respectively (left panel). (Right panel) Luciferase reporter assays. *p53*-deficient H1299 cells were co-transfected with pcDNA3, FLAG-p53 or FLAG-p53ΔC expression plasmid, p53-responsive luciferase reporter (*$p21^{WAF1}$*, *MDM2* or *Bax*) and *Renilla* luciferase cDNA. Forty-eight hours after transfection, luciferase activities were measured. (C) Colony formation assay. Forty-eight hours after transfection, SK-N-AS cells were transferred to fresh medium containing G418 (400 μg/ml). Sixteen days after selection with G418, drug-resistant colonies were stained with Giemsa's solution (left panel) and the number of colonies was scored (right panel).

whereas FLAG-p53ΔC was largely expressed in cytoplasm. Next, we examined transcriptional potential of p53ΔC in SK-N-AS cells. As seen in left panel of Fig. 3B, FLAG-p53 but not FLAG-p53ΔC was phosphorylated at Ser-15. Consistent with these results, FLAG-p53 transactivated *$p21^{WAF1}$* and *p53AIP1*. In contrast, FLAG-p53ΔC failed to transactivate *$p21^{WAF1}$* and *p53AIP1*. Similar results were also obtained by luciferase reporter assays (Fig. 3B, right panel). To examine effects of COOH-terminal deletion on pro-apoptotic activity of p53, we performed colony formation assays. SK-N-AS cells were transfected with empty plasmid, FLAG-p53 or FLAG-p53ΔC expression plasmid and maintained in medium containing G418 for 16 days. As shown in Fig. 3C, number of drug-resistant colonies was significantly reduced in cells expressing FLAG-p53. Intriguingly, enforced expression of FLAG-p53ΔC resulted in a decrease in number of drug-resistant colonies but to a lesser degree as compared with that in cells expressing FLAG-p53. These observations suggest that COOH-terminal deletion reduces transcriptional and pro-apoptotic activities of p53.

Discussion

In this study, we have identified p53ΔC in SK-N-AS cells. Consistent with the recent report [13], p53 was predominantly expressed in cytoplasm of SK-N-AS cells. According to their results, Parc inhibited p53 nuclear translocation through the direct interaction with its COOH-terminal region. Since p53 contains three NLSs in its COOH-terminal region, Parc might inhibit its nuclear access by masking its NLSs [13]. In accordance with these findings, p53 COOH-terminal peptide inhibited its cytoplasmic retention [12]. Based on our immunoprecipitation experiments, wild-type p53 but not p53ΔC was co-immunoprecipitated with the endogenous Parc in SK-N-AS cells (data not shown), suggesting that cytoplasmic retention of p53ΔC is regulated in a Parc-independent manner. p53ΔC lacks NLS II and III but retains NLS I. Although Kim et al. described that importin-α interacts with NLS I of p53 and mediates its nuclear import [18], NLS II and/or III might play a major role in nuclear import of p53 in SK-N-AS cells.

p53 phosphorylation is significantly associated with its pro-apoptotic function [4]. Exogenously expressed wild-type p53 but not p53ΔC was phosphorylated at Ser-15 in SK-N-AS cells without DNA damage and transactivated *$p21^{WAF1}$* and *p53AIP1*. Rodicker and Putzer described that exogenously expressed p53 is phosphorylated at Ser-15 without DNA damage [19]. Although it is unknown why exogenously expressed p53 but not p53ΔC is phosphorylated at Ser15 without DNA damage, it might be at least

in part due to its cytoplasmic retention. Colony formation assays demonstrated that wild-type p53 markedly reduces number of drug-resistant colonies in SK-N-AS cells, suggesting that there might not exist functional disruptions of downstream mediators of p53 in SK-N-AS cells. In response to CDDP, SH-SY5Y cells underwent apoptosis in association with a significant induction of p53. On the other hand, SK-N-AS cells did not undergo apoptosis in response to CDDP, suggesting that *p53* status might determine neuroblastoma cell fate to survive or to die. Intriguingly, CDDP treatment of SK-N-AS cells induced an accumulation of S-phase cells accompanied with up-regulation of $p21^{WAF1}$. Since p53ΔC failed to transactivate $p21^{WAF1}$ and CDDP had undetectable effects on *p73* and *p63* (other members of *p53* family) (data not shown), CDDP-mediated up-regulation of $p21^{WAF1}$ in SK-N-AS cells is regulated in a p53 family-independent manner. Knudsen et al. reported that CDDP-mediated DNA damage induces an intra-S-phase cell cycle arrest, which is correlated with a protection against apoptosis [20]. Thus, the genome maintenance system might delay the onset of mitosis, and thereby providing time to complete DNA repair and/or DNA replication before cell division in SK-N-AS cells. Further efforts should be necessary to address this issue.

Majority of *p53* mutations is detected within its DNA-binding region [21]. SK-N-AS cells have been believed to express wild-type p53 [22]. Much of information regarding *p53* mutations was derived from sequence analysis of exons 5–8 which encode its DNA-binding domain [4]. Indeed, there exist missense mutations in p53 oligomerization domain [23]. According to their results, Leu to Pro substitution at 344 inhibited the oligomerization of p53 and abolished its DNA-binding activity. Since p53ΔC lacks a part of oligomerization domain including Leu-344, p53ΔC might exist as a monomeric latent form. Recently, Bourdon et al. described that human *p53* is expressed as multiple isoforms including p53β and p53γ [24]. Based on amino acid sequence comparison, p53ΔC was distinct from p53β and p53γ (data not shown). During the preparation of our manuscript, Goldschneider et al. reported that SK-N-AS cells express p53β [25]. This discrepancy might be attributed to co-expression of p53β and p53ΔC in SK-N-AS cells and/or due to the acquired heterogeneity of SK-N-AS cells during culture. Additionally, murine *p53* expresses an alternative splicing isoform termed ASp53 with different COOH-terminus from that of wild-type p53 [26]. ASp53 displays an enhanced transcriptional activity as compared with wild-type p53, indicating that p53ΔC is distinct from human counterpart of ASp53.

Acknowledgments

This work was supported in part by a Grant-in-Aid from the Ministry of Health, Labor and Welfare for Third Term Comprehensive Control Research for Cancer, a Grant-in-Aid for Scientific Research on Priority Areas from the Ministry of Education, Culture, Sports, Science and Technology, Japan, a Grant-in-Aid for Scientific Research from Japan Society for the Promotion of Science, and a Grant from Uehara Memorial Foundation.

References

[1] M. Hollstein, D. Sidransky, B. Vogelstein, H. Harris, p53 mutations in human cancers, Science 253 (1991) 49–53.
[2] A.J. Levine, J. Momand, C.A. Finlay, The p53 tumour suppressor gene, Nature 351 (1991) 453–456.
[3] L.A. Donehower, M. Harvey, B.L. Slagle, M.J. McArthur, C.A. Montgomery Jr., J.S. Butel, A. Bradley, Mice deficient for p53 are developmentally normal but susceptible to spontaneous tumours, Nature 356 (1992) 215–221.
[4] K.H. Vousden, X. Lu, Live or let die: the cells response to p53, Nat. Rev. Cancer 2 (2002) 594–604.
[5] Y. Haupt, R. Maya, A. Kazaz, M. Oren, Mdm2 promotes the rapid degradation of p53, Nature 387 (1997) 296–299.
[6] M.H.G. Kubbutat, S.N. Jones, K.H. Vousden, Regulation of p53 stability by Mdm2, Nature 387 (1997) 299–303.
[7] G. Shaulsky, N. Goldfinger, A. Ben-Ze'ev, V. Rotter, Nuclear accumulation of p53 protein is mediated by several nuclear localization signals and plays a role in tumorigenesis, Mol. Cell. Biol. 10 (1990) 6565–6577.
[8] S.H. Liang, D. Hong, M.F. Clarke, Cooperation of a single lysine mutation and a C-terminal domain in the cytoplasmic sequestration of the p53 protein, J. Biol. Chem. 273 (1998) 19817–19821.
[9] K. Vogan, M. Bernstein, J.M. Leclerc, L. Brisson, J. Brossard, G.M. Brodeur, J. Pelletier, P. Gros, Absence of p53 gene mutations in primary neuroblastomas, Cancer Res. 53 (1993) 5269–5273.
[10] U.M. Moll, M. LaQuaglia, J. Benard, G. Riou, Wild-type p53 protein undergoes cytoplasmic sequestration in undifferentiated neuroblastomas but not in differentiated tumors, Proc. Natl. Acad. Sci. USA 92 (1995) 4407–4411.
[11] U.M. Moll, A.G. Ostermeyer, R. Haladay, B. Winkfield, M. Frazier, G. Zambetti, Cytoplasmic sequestration of wild-type p53 protein impairs the G1 checkpoint after DNA damage, Mol. Cell. Biol. 16 (1996) 1126–1137.
[12] A.G. Ostermeyer, E. Runko, B. Winkfield, B. Ahn, U.M. Moll, Cytoplasmically sequestrated wild-type p53 protein in neuroblastoma is relocated to the nucleus by a C-terminal peptide, Proc. Natl. Acad. Sci. USA 93 (1996) 15190–15194.
[13] A.Y. Nikolaev, M. Li, N. Puskas, J. Qin, W. Gu, Parc: A cytoplasmic anchor for p53, Cell 112 (2003) 29–40.
[14] A.M. Snijders, N. Nowak, R. Segraves, S. Blackwood, N. Brown, J. Conroy, G. Hamilton, A.K. Hindle, B. Huey, K. Kimura, S. Law, K. Myambo, J. Palmer, B. Yistra, J.P. Yue, J.W. Gray, A.N. Jain, D. Pinkel, D.G. Albertson, Assembly of microarrays for genome-wide measurement of DNA copy number, Nat. Genet. 29 (2001) 263–264.
[15] J.M. Nigro, A. Misra, L. Zhang, I. Smimov, H. Colman, C. Griffin, N. Ozburn, M. Chen, E. Pan, D. Koul, W.K. Yung, B.G. Feuerstein, K.D. Aldape, Integrated array-comparative genomic hybridization and expression array profiles identity clinically relevant molecular subtypes of glioblastoma, Cancer Res. 65 (2005) 1678–1686.
[16] D.L. Coppock, A.B. Pardee, Control of thymidine kinase mRNA during the cell cycle, Mol. Cell. Biol. 7 (1987) 2925–2932.
[17] R. Hamanaka, M.R. Smith, P.M. O'Connor, S. Maloid, K. Mihalic, J.L. Spivak, D.L. Longo, D.K. Ferris, Polo-like kinase is a cell cycle-regulated kinase activated during mitosis, J. Biol. Chem. 270 (1995) 21086–21091.
[18] I.S. Kim, D.H. Kim, S.M. Han, M.U. Chin, H.J. Nam, H.P. Cho, S.Y. Choi, B.J. Song, E.R. Kim, Y.S. Bae, Y.H. Moon, Truncated form of importin α identified in breast cancer cell inhibits nuclear import of p53, J. Biol. Chem. 275 (2000) 23139–23145.

[19] F. Rodicker, B.M. Putzer, p73 is effective in p53-null pancreatic cancer cells resistant to wild-type TP53 gene replacement, Cancer Res. 63 (2003) 2737–2741.
[20] K.E. Knudsen, D. Booth, S. Naderi, Z. Sever-Chroneos, A.F. Fribourg, C. Hunton, J.R. Feramisco, J.Y.J. Wang, E.S. Knudsen, RB-dependent S-phase response to DNA damage, Mol. Cell. Biol. 20 (2000) 7751–7763.
[21] M. Hollstein, M. Hergenhahn, Q. Yang, H. Bartsch, Z.Q. Wang, P. Hainaut, New approaches to understanding p53 gene tumor mutation spectra, Mutat. Res. 431 (1999) 199–209.
[22] M. Kaghad, H. Bonnet, A. Yang, L. Creancier, J.C. Biscan, A. Valent, A. Minty, P. Chalon, J.M. Lelias, X. Dumont, P. Ferrara, F. McKeon, D. Caput, Monoallelically expressed gene related to p53 at 1p36, a region frequently deleted in neuroblastoma and other human cancers, Cell 90 (1997) 809–819.
[23] M.E. Lomax, D.M. Barnes, T.R. Hupp, S.M. Picksley, R.S. Camplejohn, Characterization of p53 oligomerization domain mutations isolated from Li-Fraumeni and Li-Fraumeni like family members, Oncogene 17 (1998) 643–649.
[24] J.C. Bourdon, K. Fernandes, F. Murray-Zmijewski, G. Liu, A. Diot, D.P. Xirodimas, M.K. Saville, D.L. Lane, p53 isoforms can regulates p53 transcriptional activity, Genes Dev. 19 (2005) 2122–2137.
[25] D. Goldschneider, E. Horvilleur, L.F. Plassa, M. Guillaud-Bataille, K. Million, E. Wittmer-Dupret, G. Danglot, H. de The, J. Benard, E. May, S. Douc-Rasy, Expression of C-terminal deleted p53 isoforms in neuroblastoma, Nucleic Acids Res. 34 (2006) 5603–5612.
[26] N. Arai, D. Nomura, K. Yokota, D. Wolf, E. Brill, O. Shohat, V. Rotter, Immunologically distinct p53 molecules generated by alternative splicing, Mol. Cell. Biol. 6 (1986) 3232–3239.

THE JOURNAL OF BIOLOGICAL CHEMISTRY VOL. 282, NO. 25, pp. 18365–18376, June 22, 2007

Stabilization of p73 by Nuclear IκB Kinase-α Mediates Cisplatin-induced Apoptosis*

Received for publication, November 13, 2006, and in revised form, April 23, 2007 Published, JBC Papers in Press, April 23, 2007. DOI 10.1074/jbc.M610522200

Kazushige Furuya[‡§], Toshinori Ozaki[‡], Takayuki Hanamoto[‡], Mitsuchika Hosoda[‡], Syunji Hayashi[‡], Philip A. Barker[¶], Kunio Takano[§], Masahiko Matsumoto[§], and Akira Nakagawara[‡1]

From the [‡]Division of Biochemistry, Chiba Cancer Center Research Institute, Chiba 260-8717, Japan, the [§]Second Department of Surgery, Yamanashi University School of Medicine, Yamanashi 409-3898, Japan, and the [¶]Montreal Neurological Institute, McGill University, Montreal, Quebec H3A 2B4, Canada

In response to DNA damage, p53 and its homolog p73 have a function antagonistic to NF-κB in deciding cell fate. Here, we show for the first time that p73, but not p53, is stabilized by physical interaction with nuclear IκB kinase (IKK)-α to enhance cisplatin (CDDP)-induced apoptosis. CDDP caused a significant increase in the amounts of nuclear IKK-α and p73α in human osteosarcoma-derived U2OS cells. Ectopic expression of IKK-α prolonged the half-life of p73 by inhibiting its ubiquitination and thereby enhancing its transactivation and pro-apoptotic activities. Consistent with these results, small interfering RNA-mediated knockdown of endogenous IKK-α inhibited the CDDP-mediated accumulation of p73α. The kinase-deficient mutant form of IKK-α interacted with p73α, but failed to stabilize it. Furthermore, CDDP-mediated accumulation of endogenous p73α was not detected in mouse embryonic fibroblasts (MEFs) prepared from IKK-α-deficient mice, and CDDP sensitivity was significantly decreased in IKK-α-deficient MEFs compared with wild-type MEFs. Thus, our results strongly suggest that the nuclear IKK-α-mediated accumulation of p73α is one of the novel molecular mechanisms to induce apoptotic cell death in response to CDDP, which may be particularly important in killing tumor cells with *p53* mutation.

The NF-κB signaling pathway is activated by a variety of structurally and functionally unrelated stimuli, including inflammatory cytokines, ionizing radiation, viral and bacterial infection, and oxidative stress (reviewed in Refs. 1 and 2). Under normal conditions, NF-κB exists as heterodimeric complexes composed of p50 and p65 (RelA) subunits and is kept transcriptionally inactive through interaction with its inhibitory proteins such as IκB-α and IκB-β. IκB proteins mask the nuclear localization signal of NF-κB, thereby preventing its nuclear translocation. Upon certain stimulations, IκB proteins are rapidly phosphorylated at specific serine residues in the N-terminal their signal-responsive domain by upstream regulator IκB kinase (IKK)[2] complex and subsequently polyubiquitinated and degraded in a proteasome-dependent manner (reviewed in Ref. 3). The high molecular mass IKK complex comprises two related catalytic subunits, IKK-α (also called IKK-1) and IKK-β (also called IKK-2), and one regulatory subunit with a scaffold function, IKK-γ (also called NEMO) (reviewed in Ref. 3). The proteolytic degradation of IκB proteins exposes the nuclear localization signal of NF-κB and results in translocation of NF-κB from the cytoplasm to the nucleus, allowing it to participate in transcriptional regulation of numerous target genes involved in immune responses, inflammatory reactions, cell adhesion, cell proliferation, apoptotic cell death, and other cellular processes. Therefore, the IKK complex represents one of the critical upstream regulators of the NF-κB signaling pathway.

In many experimental systems, the activation of NF-κB has been shown to play an important role in the control of survival processes, protecting cells from a variety of apoptotic signals (4–8). For example, tumor necrosis factor-α (TNF-α) simultaneously activates the NF-κB-mediated cellular protective mechanism against the pro-apoptotic effect of TNF-α through the induction of the NF-κB-responsive genes that function to block apoptosis. Additionally, inhibition of NF-κB has been shown to enhance sensitivity to chemotherapeutic agents (9, 10). Consistent with the well documented anti-apoptotic effect of NF-κB, high levels of NF-κB activity are detectable in various human tumors (11). On the other hand, NF-κB activation results in the promotion of apoptosis, depending on different stimuli and cell types. Huang and Fan (12) reported that the activation of NF-κB contributes to paclitaxel-induced apoptosis in human solid tumor cells. In addition, Bian *et al.* (13) found that NF-κB activation mediates doxorubicin-induced apoptosis in N-type neuroblastoma cells. In both cases, treatment of cells with the cytotoxic agents significantly down-regulated cytoplasmic IκB-α and then promoted the nuclear transloca-

* This work was supported in part by a grant-in-aid for third term comprehensive control research for cancer from the Ministry of Health, Labor and Welfare, by a grant-in-aid for scientific research on priority areas from the Ministry of Education, Culture, Sports, Science and Technology of Japan, and by a grant-in-aid for scientific research from the Japan Society for the Promotion of Science. The costs of publication of this article were defrayed in part by the payment of page charges. This article must therefore be hereby marked "*advertisement*" in accordance with 18 U.S.C. Section 1734 solely to indicate this fact.

[1] To whom correspondence should be addressed: Div. of Biochemistry, Chiba Cancer Center Research Inst., 666-2 Nitona, Chuoh-ku, Chiba 260-8717, Japan. Tel.: 81-43-264-5431; Fax: 81-43-265-4459; E-mail: akiranak@chiba-cc.jp.

[2] The abbreviations used are: IKK, IκB kinase; TNF-α, tumor necrosis factor-α; CDDP, cisplatin; siRNA, small interfering RNA; MEFs, mouse embryonic fibroblasts; MTT, 3-(4,5-dimethylthiazol-2-yl)-2,5-diphenyltetrazolium bromide; RT, reverse transcription; GST, glutathione *S*-transferase; HA, hemagglutinin; PIPES, 1,4-piperazinediethanesulfonic acid; MOPS, 4-morpholinepropanesulfonic acid; CBP, cAMP-responsive element-binding protein-binding protein.

tion of NF-κB; however, the molecular mechanism of the pro-apoptotic effect of NF-κB is still largely unknown.

p73 belongs to a small family of p53-related nuclear transcription factors. In accordance with their structural similarity, p73 functions in a manner analogous to p53 by inducing G_1 cell cycle arrest or apoptosis in certain cancerous cells through transactivating an overlapping set of p53/p73 target genes (reviewed in Ref. 14). Like p53, endogenous p73 becomes stabilized as well as activated in cells exposed to certain genotoxic stimuli, including γ-irradiation and cisplatin (CDDP), and contributes to an apoptotic response to DNA damage (15–17). p73 is expressed as multiple isoforms that differ at their N and C termini, arising from alternative splicing and promoter usage (reviewed in Ref. 14). Among them, an N-terminally truncated form of p73 (ΔNp73) that lacks the transactivation domain of p73 has an oncogenic potential and exhibits dominant-negative behavior toward wild-type p73 as well as p53 (18–20). Of particular note, we (22) and others (21, 23) demonstrated that p73 directly transactivates the expression of its own negative regulator, ΔNp73, suggesting that a negative feedback regulation of p73 by ΔNp73 exists to modulate cell survival and death.

In response to primary antigenic stimulation, NF-κB limits the up-regulation of pro-apoptotic p73 in T cells, resulting in the promotion of T cell survival; however, the precise molecular basis by which NF-κB activation inhibits the expression of p73 remains to be determined (24). It is worth noting that IKK-β, but not IKK-α, activates NF-κB, thereby inhibiting the accumulation of p53 at the protein level in response to the anticancer agent doxorubicin (25). IκB-α might play a role in sequestering p53 in the cytoplasm through the physical interaction with p53, thereby preventing the nuclear translocation of p53 (26). These observations suggest that NF-κB activation might abrogate p53- and/or p73-mediated apoptosis. In marked contrast, Ryan *et al.* (27) reported that NF-κB is required for p53-dependent apoptosis. Additionally, it has been demonstrated that p53 is a direct transcriptional target of NF-κB and that the p53-activating signal is partially blocked by inhibition of NF-κB activation (28–30). In support of this notion, Fujioka *et al.* (31) reported that NF-κB acts as a pro-apoptotic factor by activating the p53 signaling pathway. However, the functional significance of the possible interplay between the NF-κB signaling pathway and p53- and/or p73-mediated apoptosis has not been established.

In addition to the role of the cytoplasmic IKK complex in regulating the signal-dependent induction of NF-κB target genes, Birbach *et al.* (32) found that one of its components (IKK-α) shuttles between the cytoplasm and nucleus of unstimulated cells, suggesting that IKK-α might have a novel nuclear role in controlling cell survival and death. Consistent with this notion, it has been shown that IKK-α accumulates in the cell nucleus in response to cytokine exposure and stimulates the expression of NF-κB-responsive genes through promoter-associated histone H3 phosphorylation (33, 34). In this study, we found that IKK-α accumulates in the cell nucleus during the CDDP-mediated apoptotic process. Moreover, IKK-α increased the stability of p73, but not p53, through direct interaction with p73 and enhanced p73-dependent transcriptional activity as well as pro-apoptotic function. Reduction of endogenous IKK-α by small interfering RNA (siRNA) against IKK-α resulted in the significant attenuation of the CDDP-induced accumulation of p73α. Similar results were also obtained in mouse embryonic fibroblasts (MEFs) derived from IKK-α-deficient mice (IKK-$\alpha^{-/-}$ MEFs). Thus, our findings suggest that IKK-α has a novel nuclear role in regulating DNA damage-induced apoptosis, which is distinct from its cytoplasmic role in activating NF-κB.

EXPERIMENTAL PROCEDURES

Cell Lines and Transfection—African green monkey kidney COS-7 cells and human osteosarcoma U2OS cells were maintained in Dulbecco's modified Eagle's medium, 10% fetal bovine serum, penicillin, and streptomycin (Invitrogen). Human lung carcinoma H1299, human neuroblastoma SK-N-AS, and mouse fibrosarcoma L929 cells were grown in RPMI 1640 medium, 10% fetal bovine serum, penicillin, and streptomycin. COS-7 cells were transfected with FuGENE 6 (Roche Applied Science) in accordance with the manufacturer's specifications. H1299 and U2OS cells were transfected with Lipofectamine (Invitrogen) according to the manufacturer's instructions. pcDNA3 (Invitrogen) was used as a blank plasmid to balance the amount of DNA introduced in transient transfection.

Cell Survival Assay—U2OS cells were seeded at 5×10^3/well in a 96-well tissue culture dish with 100 μl of complete medium and allowed to attach overnight. CDDP was added to the cultures at a final concentration of 20 μM, and cell viability was determined by a modified 3-(4,5-dimethylthiazol-2-yl)-2,5-diphenyltetrazolium bromide (MTT) assay at the indicated time points after the addition of CDDP as described (22).

RNA Extraction and Reverse Transcription (RT)-PCR—Total RNA was prepared from U2OS cells exposed to CDDP (20 μM) using an RNeasy mini kit (Qiagen Inc.) according to the manufacturer's protocol. For the RT-PCR, first-strand cDNA was generated using SuperScript II reverse transcriptase (Invitrogen) and random primers. PCR amplification was performed with r*Taq* DNA polymerase (Takara, Ohtsu, Japan).[3] The expression of glyceraldehyde-3-phosphate dehydrogenase was measured as an internal control.

Plasmids—The protein-coding region of IKK-α was amplified by PCR and inserted between the EcoRI and XhoI sites of pcDNA3-FLAG. The K44A mutation was introduced into wild-type IKK-α using PfuUltra™ high fidelity DNA polymerase (Stratagene) according to the manufacturer's instructions. The nucleotide sequence of the PCR product was determined to verify the presence of the desired mutation and the absence of random mutations.

Immunoblotting, Immunoprecipitation, and Glutathione S-Transferase (GST) Pulldown Assay—For immunoblotting, cell lysates (50 μg of protein) were analyzed using anti-FLAG monoclonal antibody M2 (Sigma); anti-hemagglutinin (HA) monoclonal antibody (12CA5, Roche Applied Biosciences); anti-p73 monoclonal antibody (Ab-4, NeoMarkers, Fremont, CA); anti-p53 monoclonal antibody (DO-1, Oncogene Research Products, Cambridge, MA); anti-Bax monoclonal antibody (6A7, eBioscience, San Diego, CA); anti-IKK-α polyclonal (M-280), anti-IKK-β polyclonal (H-470), anti-IKK-γ

[3] The list of primer sets used is available upon request.

polyclonal (FL-417), anti-p65 polyclonal (C-20), anti-IκB-α polyclonal (C-21), or polyclonal anti-$p21^{WAF1}$ (H-164) antibody (Santa Cruz Biotechnology, Inc., Santa Cruz, CA); or anti-actin polyclonal antibody (20–33, Sigma). After incubation with primary antibodies, membranes were incubated with horseradish peroxidase-conjugated secondary antibodies (Cell Signaling Technology, Beverly, MA), and immunoreactive proteins were finally visualized by the ECL system (Amersham Biosciences AB, Uppsala, Sweden). For immunoprecipitation, cell lysates were precleared with 30 μl of protein G-Sepharose suspension (Amersham Biosciences AB) and then incubated with anti-HA polyclonal antibody (Medical and Biological Laboratories, Nagoya, Japan) or anti-FLAG monoclonal antibody for 2 h at 4 °C. Immunoblotting was performed with anti-FLAG or anti-p73 monoclonal antibody as described above. For GST pulldown assay, [^{35}S]methionine-labeled FLAG-IKK-α was generated in the coupled transcription/translation system (Promega, Madison, WI) and mixed with GST or GST-p73 fusion proteins coupled to glutathione-Sepharose (Amersham Biosciences AB) for 2 h at 4 °C. ^{35}S-Labeled bound proteins were analyzed by 10% SDS-PAGE and visualized by autoradiography.

Subcellular Fractionation and Immunofluorescence Analysis—To prepare nuclear and cytoplasmic extracts, cells were lysed in 10 mM Tris-HCl (pH 7.5), 1 mM EDTA, 0.5% Nonidet P-40, 1 mM phenylmethylsulfonyl fluoride, and a protease inhibitor mixture (Sigma) and centrifuged at 5000 rpm for 10 min to collect soluble fractions, which are referred to as cytosolic extracts. Insoluble materials were washed with the lysis buffer and further dissolved in SDS sample buffer to collect the nuclear extracts. The nuclear and cytoplasmic fractions were subjected to immunoblot analysis using anti-lamin B monoclonal antibody (Ab-1; Oncogene Research Products) or anti-α-tubulin monoclonal antibody (DM1A, Cell Signaling Technology). For indirect immunofluorescence, U2OS cells were grown on coverslips and transfected with the indicated expression plasmids. Forty-eight hours after transfection, cells were fixed in 100% methanol for 20 min at −20 °C, blocked in 3% bovine serum albumin, stained with the corresponding antibodies, and examined with a laser scanning confocal microscope (Olympus, Tokyo, Japan). Nuclear matrix fractionation was performed as described previously (35, 36). In brief, cells were washed with ice-cold phosphate-buffered saline and lysed in 10 mM PIPES (pH 6.8), 100 mM NaCl, 300 mM sucrose, 3 mM $MgCl_2$, 1 mM EGTA, 1 mM dithiothreitol, and 0.5% Triton X-100 containing a protease inhibitor mixture, and insoluble materials were separated from soluble proteins (fraction I) by centrifugation. The pellet fraction was treated with DNase I (at a final concentration of 1 mg/ml) for 15 min at 37 °C, and then ammonium sulfate was added to the reaction mixture (at a final concentration of 0.25 M). The pellet fraction was separated from the supernatant (fraction II) by centrifugation and further extracted with 2 M NaCl (fraction III). The remaining pellet was solubilized in 8 M urea, 0.1 M NaH_2PO_4, and 10 mM Tris-HCl (pH 8.0) to give fraction IV.

Protein Stability and Ubiquitination Assays—COS-7 cells were transfected with HA-p73α with or without IKK-α. Cells were harvested at different time points after pretreatment with cycloheximide (100 μg/ml), and cell lysates were processed for immunoblot analysis with anti-p73 or anti-actin antibody. Densitometry was used to quantify the amounts of HA-p73α that normalized to actin. Ubiquitination assay was performed as described previously (37). COS-7 cells were cotransfected with HA-p73α and His-tagged ubiquitin with or without IKK-α. Forty hours after transfection, cells were exposed to the proteasomal inhibitor MG132 (20 μM) for 6 h. Cells were resuspended in 6 M guanidine HCl, 0.1 M Na_2HPO_4/NaH_2PO_4 (pH 8.0), and 10 mM imidazole, and ubiquitinated materials were recovered by nickel-nitrilotriacetic acid-agarose beads (Qiagen Inc.) and analyzed by immunoblotting with anti-HA antibody.

Luciferase Reporter and Apoptosis Assays—p53-deficient H1299 cells on 12-well plates were cotransfected with a p53/p73-responsive element-driven luciferase reporter, an internal control vector for *Renilla* luciferase, and a combination of the indicated expression vectors. Both firefly and *Renilla* luciferase activities were assayed with the Dual-Luciferase reporter assay system (Promega). The firefly luminescence signal was normalized based on the *Renilla* luminescence signal. For apoptosis assay, H1299 cells on 6-well plates were cotransfected with β-galactosidase (50 ng) and HA-p73α (50 ng) with or without increasing amounts of IKK-α or IKK-β (100, 200, and 400 ng). Forty-eight hours after transfection, cells were stained with a 0.4% solution of trypan blue for 10 min at room temperature. Thereafter, cells were fixed in phosphate-buffered saline containing 2.5% glutaraldehyde, 1 mM $MgCl_2$, and 2 mM EGTA for 10 min and then stained with Red-Gal for 2 h as described (11). Red-Gal was used as a marker to visualize the transfected cells and to assess the apoptotic frequency among the transfectants. Apoptotic cells were scored by rounding up of cells with dark pink-purple coloration due to double staining with Red-Gal and trypan blue.

In Vitro Kinase Assay—GST or GST-p73 deletion mutants were incubated with the active form of IKK-α (Upstate Biotechnology, Lake Placid, NY) in a solution containing 40 mM MOPS-NaOH (pH 7.0), 1 mM EDTA, 25 mM sodium acetate, and 0.25 mM ATP in the presence of [γ-^{32}P]ATP at 30 °C for 10 min. After incubation, the reaction mixtures were separated by SDS-PAGE. The gel was then dried and subjected to autoradiography.

RNA Interference—To knock down endogenous IKK-α, the expression plasmid for siRNA directed against human IKK-α (GeneSuppressor, Imgenex Corp., San Diego, CA) was introduced into U2OS cells using Lipofectamine following the manufacturer's instructions. Forty-eight hours after transfection, whole cell lysates were prepared and analyzed for the expression levels of IKK-α by immunoblotting.

Chromatin Immunoprecipitation Assays—Chromatin immunoprecipitation assays were performed following a protocol provided by Upstate Biotechnology (Lake Placid, NY). In brief, cells were cross-linked with 1% formaldehyde in medium for 10 min at 37 °C. Chromatin solutions were prepared and immunoprecipitated with anti-HA antibody. DNAs of the immunoprecipitates and control input DNAs were purified using a QIAquick PCR purification kit (Qiagen Inc.) and then analyzed by regular PCR using human *Bax* promoter-specific

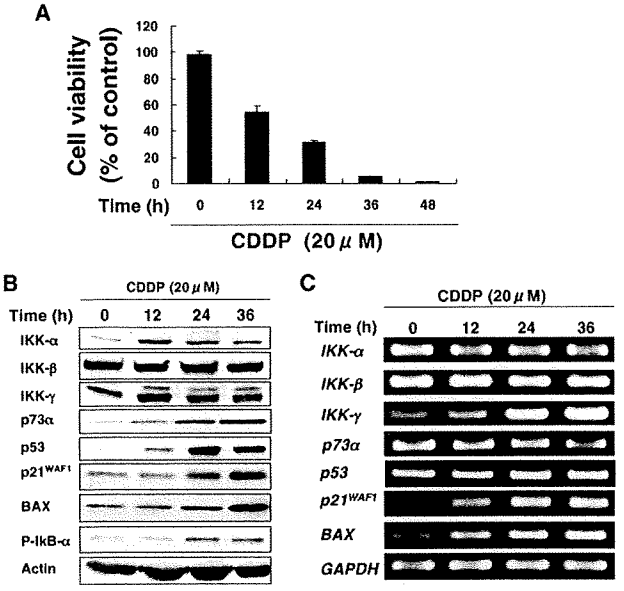

FIGURE 1. **Induction of IKK-α in response to CDDP.** *A*, effect of CDDP on osteosarcoma-derived U2OS cell survival. At the indicated time points after treatment with CDDP (at a final concentration of 20 μM), cell viability was determined by MTT assays. *B*, immunoblot analysis. At the indicated time periods after treatment with CDDP, whole cell lysates were prepared and subjected to immunoblotting with the indicated antibodies. For p73α, whole cell lysates were subjected to immunoprecipitation with anti-p73 antibody, followed by immunoblotting with anti-p73 antibody. Actin expression served as a control for equal loading of proteins in each lane. *C*, RT-PCR analysis. Total RNA was extracted from U2OS cells at the indicated times after CDDP treatment and used for RT-PCR with the indicated primers. Glyceraldehyde-3-phosphate dehydrogenase (*GAPDH*) was used as a control.

primers. The primer sequences used were 5′-AGGCTGAGACG-GGGTTATCT-3′ and 5′-AAAGCTCAGAGGCCCAAAAT-3′.

RESULTS

Induction of IKK-α during CDDP-mediated Apoptosis in U2OS Cells—To define the potential function(s) of IKKs in DNA damage-induced signaling, we first examined their expression levels in human osteosarcoma-derived U2OS cells exposed to the DNA-damaging chemotherapeutic drug CDDP. Under our experimental conditions, U2OS cells underwent apoptosis in a time-dependent manner as examined by cell survival assays (Fig. 1*A*). Similar results were also obtained by fluorescence-activated cell sorter analysis (data not shown). Immunoblot analysis demonstrated that p53 and its homolog p73α, which are major mediators in the DNA damage response (reviewed in Refs. 14 and 38), were significantly induced at protein levels in response to CDDP (Fig. 1*B*), whereas the expression of *p53* and *p73α* mRNAs remained unchanged (Fig. 1*C*). Their accumulation was associated with several of their downstream effectors, including $p21^{WAF1}$ and Bax. Notably, CDDP treatment led to a remarkable accumulation of IKK-α, and its induction was observed between 12 and 36 h after exposure to CDDP (Fig. 1*B*). Twelve hours after treatment with CDDP, the amount of IKK-γ (NEMO) was transiently increased at the protein level. By contrast, the amount of IKK-β was not significantly altered upon CDDP treatment.

RT-PCR analysis revealed that the expression levels of *IKK-α* and *IKK-β* mRNAs remained unchanged regardless of CDDP treatment, whereas a marked increase in the expression level of *IKK-γ* mRNA was detected in a time-dependent manner in response to CDDP (Fig. 1*C*). Intriguingly, immunoblot analysis also demonstrated that CDDP treatment caused a significant increase in the phosphorylated form of IκB-α, which is a well characterized substrate for the IKK complex (reviewed in Ref. 3). Taken together, these results suggest that DNA damage-induced accumulation of both p53 and p73α is associated with the up-regulation of IKK-α and IKK-γ and that a functional interaction might exist between them in DNA damage-mediated apoptotic pathways.

Nuclear Accumulation of IKK-α in Response to CDDP—It was shown recently that IKK-α shuttles between the nucleus and cytoplasm in a CRM1-dependent fashion (32). Nuclear IKK-α has the ability to transactivate NF-κB-responsive genes that control survival pathways after cytokine exposure (33, 34). In addition, Verma *et al.* (39) found that, like IKK-α, IKK-γ is present in both the nucleus and cytoplasm. These observations prompted us to examine whether the subcellular localization of endogenous IKKs can change in response to CDDP. For this purpose, nuclear and cytoplasmic extracts were prepared from U2OS cells exposed to CDDP or left untreated and then subjected to immunoblotting with the indicated antibodies. In agreement with previous results (33), IKK-α was localized in both the nucleus and cytoplasm, whereas IKK-β was expressed almost exclusively in the cytoplasm (Fig. 2*A*). The amounts of cytoplasmic IKK-α, IKK-β, and IKK-γ remained unchanged regardless of the treatment with CDDP. Of note, CDDP treatment led to a remarkable accumulation of IKK-α in the cell nucleus in a time-dependent manner, whereas IKK-β accumulated in the cell nucleus to a lesser degree. The temporal patterns of CDDP-mediated accumulation of nuclear IKK-α correlated with those of p73α. On the other hand, the transient nuclear accumulation of IKK-γ was detected 12 h after exposure to CDDP. Compared with the levels of nuclear IKK-α accumulated in response to CDDP, the amount of nuclear IKK-γ was small. Consistent with the enhanced phosphorylation of IκB-α in response to CDDP, cytoplasmic IκB-α was decreased in a time-dependent manner. However, CDDP treatment had little or no effect on the nuclear accumulation of the NF-κB p65 subunit (RelA), indicating that nuclear translocation of p65 might be inhibited in the presence of CDDP. Considering that, among IKKs, CDDP treatment promoted a significant nuclear accumulation of IKK-α, it is likely that IKK-α might have a certain nuclear function during CDDP-mediated apoptosis.

To investigate whether exogenously expressed IKK-α can reflect the behavior of endogenous IKK-α, we examined the intracellular distribution of exogenous IKK-α by immunoblotting and immunofluorescence staining. Nuclear and cytoplasmic fractions were prepared from U2OS cells transfected with the expression plasmid for FLAG-IKK-α or HA-p73α and subjected to immunoblotting with anti-FLAG or anti-p73α antibody, respectively. As shown in Fig. 2*B*, HA-p73α was localized exclusively in the cell nucleus, whereas FLAG-IKK-α was present in both the nucleus and cytoplasm. Surprisingly, immunofluorescence staining with anti-FLAG and anti-lamin B antibodies clearly showed that exogenous IKK-α was localized in

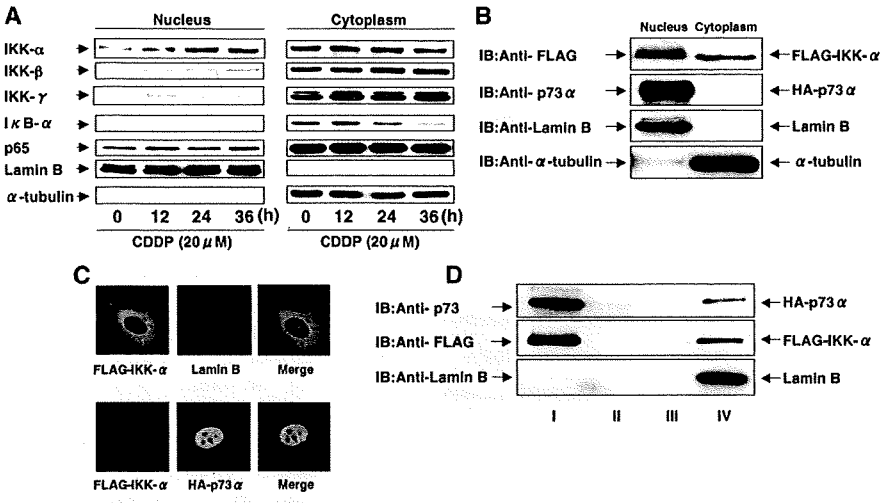

FIGURE 2. **Nuclear accumulation of IKK-α.** *A*, nuclear accumulation of IKK-α in response to CDDP. At the indicated time periods after the addition of CDDP, U2OS cells were fractionated into nuclear and cytoplasmic fractions and then analyzed by immunoblotting with the indicated antibodies. Anti-lamin B and anti-α-tubulin immunoblotting were included to assess the purity of each fraction. *B*, subcellular localization of exogenous IKK-α. U2OS cells were transiently transfected with the expression plasmid for FLAG-IKK-α or HA-p73α. Cells were subjected to biochemical fractionation, followed by immunoblotting (*IB*) with anti-FLAG or anti-p73 antibody. *C*, co-localization of IKK-α and p73 in nuclear laminae. U2OS cells were transiently transfected with the FLAG-IKK-α expression plasmid alone (*upper panels*) or with the HA-p73α expression plasmid (*lower panels*). Cells were processed for indirect immunofluorescence and double-stained with anti-FLAG and anti-lamin B antibodies (*upper panels*) or with anti-HA and anti-FLAG antibodies (*lower panels*). The merged images show that IKK-α co-localized with p73α in nuclear laminae (*yellow*). *D*, p73α and IKK-α are detected in the nuclear matrix fraction. U2OS cells cotransfected with the expression plasmids for HA-p73α and FLAG-IKK-α were subjected to high salt nuclear matrix fractionation as described under "Experimental Procedures." Each fraction was analyzed by immunoblotting with anti-p73 (*upper panel*), anti-IKK-α (*middle panel*), or anti-lamin B (*lower panel*) antibody.

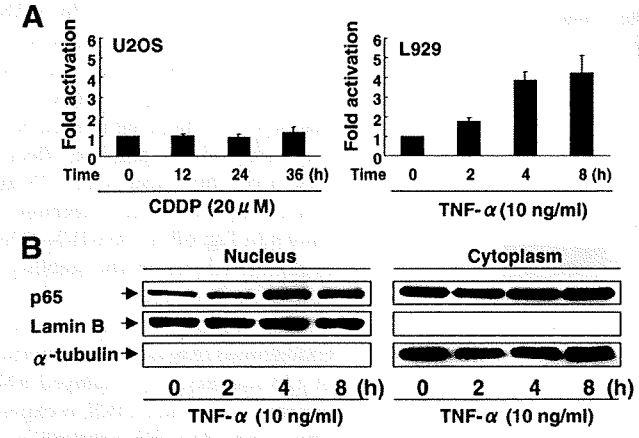

FIGURE 3. **NF-κB is not activated in response to CDDP.** *A*, U2OS (*left panel*) or L929 (*right panel*) cells were cotransfected with the NF-κB reporter construct (pELAM1-Luc) and the *Renilla* luciferase plasmid (pRL-tk). Twenty-four hours after transfection, U2OS and L929 cells were treated with CDDP and TNF-α, respectively. At the indicated time points after treatment, luciferase activity was determined. *B*, nuclear accumulation of p65 in L929 cells exposed to TNF-α. At the indicated time periods after treatment with TNF-α, L929 cells were fractionated into nuclear and cytoplasmic fractions and then analyzed directly by immunoblotting with anti-p65 antibody.

the cytoplasm and nuclear lamina, as indicated by the extensive co-localization with lamin B, a nuclear lamina marker (Fig. 2*C*). Intriguingly, HA-p73α was co-localized with FLAG-IKK-α in the nuclear lamina of the transfected cells. To confirm these observations, nuclear matrix fractionation was performed 48 h after transfection, and the fractions obtained were subjected to immunoblotting. As shown in Fig. 2*D*, HA-p73α and FLAG-IKK-α were detected in nuclear matrix fraction (fraction IV). Our results suggest that nuclear IKK-α might interact with pro-apoptotic p73α and modulate its function.

As described above, the amounts of the nuclear transactivating p65 subunit remained unchanged in U2OS cells treated with CDDP. These findings prompted us to examine whether NF-κB activation can be detected in response to CDDP. To this end, U2OS cells transfected with the NF-κB reporter plasmid (40) were treated with CDDP, and their luciferase activity was determined. Consistent with the previous observations (13), CDDP treatment did not enhance NF-κB-dependent transcriptional activation (Fig. 3*A*, *left panel*). Under our experimental conditions, NF-κB-dependent transcriptional activation was detected within 2 h of exposure to TNF-α in the mouse fibrosarcoma cell line L929 (Fig. 3*A*, *right panel*), which is widely used to investigate TNF-α-dependent NF-κB activation (41). In addition, treatment of L929 cells with TNF-α caused a nuclear accumulation of p65 (Fig. 3*B*). Thus, it is likely that, the lack of a significant effect of CDDP on NF-κB-dependent transcriptional activation could be attributed to lack of the regulated nuclear accumulation of p65.

IKK-α Interacts with p73—To determine whether IKK-α can interact with p73 in cells, whole cell lysates prepared from transfected COS-7 cells were immunoprecipitated with anti-FLAG or anti-HA antibody and analyzed by immunoblotting using anti-p73 or anti-FLAG antibody, respectively. As shown in Fig. 4*A*, exogenously expressed FLAG-IKK-α and HA-p73α formed stable complexes in COS-7 cells. Similarly, HA-p73β was co-immunoprecipitated with FLAG-IKK-α (data not shown). Their interaction was further examined using endogenous materials. As shown in Fig. 4*B*, endogenous p73α formed a protein complex with endogenous IKK-α in U2OS cells exposed to CDDP. Similar results were also obtained in HeLa cells (data not shown). In contrast, immunoprecipitation of endogenous p53 followed by immunoblotting with anti-FLAG antibody did not detect co-immunoprecipitated FLAG-IKK-α (Fig. 4*C*), indicating that IKK-α interacts with p73, but not with p53, in cells. To identify the p73 determinants involved in the interaction with IKK-α, we generated several deletion mutants of p73α fused to GST and tested their ability to bind to FLAG-IKK-α in GST pulldown assays. These mutants were designed based on p73α, including the transactivation, DNA-binding,

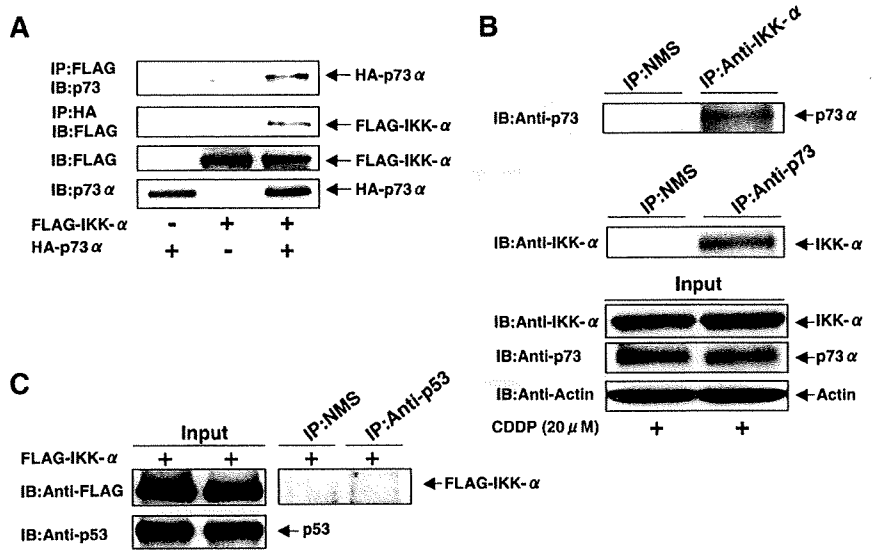

FIGURE 4. **Interaction between IKK-α and p73α.** *A*, FLAG-IKK-α was transiently coexpressed with HA-p73α in COS-7 cells as indicated. Whole cell lysates were subjected to immunoprecipitation (*IP*) with anti-FLAG or anti-HA antibody, followed by immunoblotting (*IB*) with anti-p73 or anti-FLAG antibody, respectively. *B*, whole cell lysates were prepared from U2OS cells exposed to CDDP and subjected to immunoprecipitation with normal mouse serum (*NMS*), anti-IKK-α antibody, or anti-p73 antibody, followed by immunoblotting with the indicated antibodies. *C*, FLAG-IKK-α was transiently transfected into COS-7 cells. Whole cell lysates were subjected to immunoprecipitation with normal mouse serum or anti-p53 antibody, followed by immunoblotting with anti-FLAG antibody. *Input* represents the 10% materials used for immunoprecipitation in *B* and *C*.

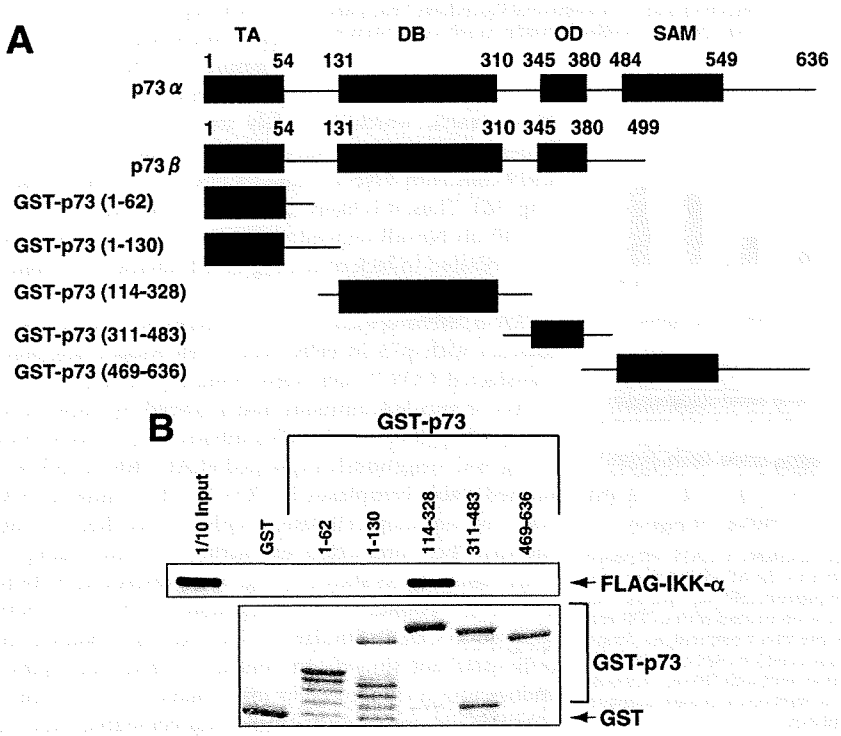

FIGURE 5. **DNA-binding domain of p73α is required for interaction with IKK-α.** *A*, shown is a schematic representation of the GST-p73 fusion proteins. *TA*, transactivation domain; *DB*, DNA-binding domain; *OD*, oligomerization domain; *SAM*, sterile α-motif domain. *B*, the DNA-binding domain of p73α is required for the interaction with IKK-α. ^{35}S-Labeled FLAG-IKK-α was incubated with GST or the indicated GST-p73 fusion proteins, and bound radiolabeled proteins were recovered on glutathione-Sepharose beads and visualized by autoradiography. The 1/10 volumes of input sample (*1/10 Input*) of ^{35}S-labeled FLAG-IKK-α used for pulldown assay were applied to the same gel (*upper panel*). Coomassie Blue-stained GST-p73 fusion proteins together with GST are also shown (*lower panel*).

oligomerization, and sterile α-motif domains (Fig. 5*A*). As shown in Fig. 5*B*, radiolabeled FLAG-IKK-α bound to GST-p73-(114–328), but not to the other GST fusion proteins. Taken together, our results suggest that IKK-α directly interacts with p73 through its DNA-binding domain.

IKK-α Increases p73 Stability—As described previously (16, 42), some p73-interacting protein kinases, including c-Abl and protein kinase Cδ, can stabilize p73. To investigate whether IKK-α can affect the stability of p73, COS-7 cells were transiently cotransfected with equal amounts of the HA-p73α expression plasmid with or without increasing amounts of the expression plasmid encoding IKK-α, and the protein level of HA-p73α was examined. As shown in Fig. 6*A*, the amount of HA-p73α was significantly increased in the presence of exogenous IKK-α, whereas IKK-α had no detectable impact on the stability of FLAG-p53. In addition, HA-p73β was also stabilized by IKK-α, but to a lesser degree compared with HA-p73α. *p73α* mRNA levels remained unchanged in the presence of IKK-α (Fig. 6*A*, *lower panels*), suggesting that IKK-α regulates p73 at the protein level. Next, we examined the possible effect of IKK-β on the stability of p73 and p53 by transient cotransfection. As shown in Fig. 6*B*, FLAG-IKK-β had negligible effects on the stability of both p73α and p53.

To investigate a possible role of endogenous IKK-α in the regulation of p73 stability, we employed RNA interference to block IKK-α expression. The enforced expression of siRNA against IKK-α in U2OS cells resulted in a significant reduction of endogenous IKK-α (Fig. 6*C*). We then tested the effect of knockdown of endogenous IKK-α on the CDDP-mediated accumulation of p73α. U2OS cells were transiently transfected with the expression plasmid for siRNA against IKK-α and exposed to CDDP for 36 h. As shown in Fig. 6*C*, down-regulation of endogenous IKK-α expression